

RECEIVED: March 8, 2022

REVISED: June 8, 2022

ACCEPTED: June 29, 2022

PUBLISHED: August 10, 2022

Scalar QED as a toy model for higher-order effects in classical gravitational scattering

Zvi Bern,^a Juan Pablo Gatica,^a Enrico Herrmann,^a Andres Luna^b and Mao Zeng^c

^a*Mani L. Bhaumik Institute for Theoretical Physics,
Department of Physics and Astronomy, University of California, Los Angeles,
475 Portola Plaza, Los Angeles, CA 90095, U.S.A.*

^b*Niels Bohr International Academy & Discovery Center,
Niels Bohr Institute, University of Copenhagen,
Blegdamsvej 17, DK-2100, Copenhagen Ø, Denmark*

^c*Higgs Centre for Theoretical Physics, University of Edinburgh,
James Clerk Maxwell Building, Edinburgh EH9 3FD, U.K.*

E-mail: bern@physics.ucla.edu, jpgatica3541@g.ucla.edu,
eh10@g.ucla.edu, andres.luna@nbi.ku.dk, mzeng@ed.ac.uk

ABSTRACT: Quantum Electrodynamics (QED) serves as a useful toy model for classical observables in gravitational two-body systems with reduced complexity due to the linearity of QED. We investigate scattering observables in scalar QED at the sixth order in the charges (two-loop order) in a classical regime analogous to the post-Minkowskian expansion in General Relativity. We employ modern scattering amplitude tools and extract classical observables by both eikonal methods and the formalism of Kosower, Maybee, and O’Connell (KMOC). In addition, we provide a simplified approach to extracting the radial action beyond the conservative sector.

KEYWORDS: Scattering Amplitudes, Classical Theories of Gravity

ARXIV EPRINT: [2112.12243](https://arxiv.org/abs/2112.12243)

Contents

1	Introduction	1
2	Review of methods	4
2.1	Classical limit of quantum scattering amplitudes — soft and potential region	4
2.2	Generalized unitarity and scalar QED scattering amplitudes up to $\mathcal{O}(\alpha^3)$	7
2.2.1	Tree-level amplitudes in scalar QED	7
2.2.2	One-loop integrand in scalar QED	9
2.2.3	Two-loop integrand in scalar QED	10
2.3	Soft and potential region expansion, IBP, and differential equations	11
2.4	Soft radial action and master integral subtraction of classically divergent terms	12
2.5	KMOC framework for classical conservative and radiative observables	15
2.5.1	Electromagnetic impulse	16
2.5.2	Radiated momentum	18
3	Conservative dynamics at $\mathcal{O}(\alpha^3)$	19
3.1	Conservative scattering amplitudes	19
3.2	Eikonal approach to classical conservative scattering	20
3.3	Conservative eikonal phase, scattering angle, and two-body Hamiltonian	21
3.4	Conservative impulse and scattering angle via KMOC	24
4	Radiative dynamics at $\mathcal{O}(\alpha^3)$	25
4.1	Radiative scattering amplitudes	25
4.2	Eikonal approach to classical scattering including radiation effects	27
4.3	Radiative impulse, energy loss, and scattering angle via KMOC	33
4.4	Radiative radial action	34
5	Conclusions	35

1 Introduction

The landmark detection of gravitational waves [1, 2] has opened a remarkable new window into the Universe that promises major new advances into black holes, neutron stars, and perhaps even provides new insights into fundamental physics. The recent experimental progress has inspired efforts to develop new theoretical tools for predicting gravitational-wave signals that meet the precision challenges of current and future detectors [3–6]. A variety of complementary tools are being used, including the effective one-body (EOB) formalism [7], numerical relativity [8–10], the self-force formalism [11, 12], as well as perturbative methods such as the post-Newtonian (PN) expansion [13, 14], the effective

field theory (EFT) known as nonrelativistic general relativity (NRGR) [15–26], as well as the post-Minkowskian (PM) expansion [27–43] and the observables based method originally devised by Kosower, Maybee, and O’Connell [44–51]. Information from various approaches can be combined into state-of-the-art results and provide nontrivial cross-checks, see e.g. refs. [40, 52–66].

The post-Minkowskian approach is a weak-field expansion in Newton’s constant, G , and has risen in prominence in recent years. It has the advantage of maintaining Lorentz invariance and gives results with exact relativistic velocity dependence. The scattering amplitude framework for post-Minkowskian calculations [37–40, 44, 48, 67] naturally meshes with this covariant approach. Calculations of scattering amplitudes have advanced enormously, making this a natural framework for state-of-the-art post-Minkowskian calculations. The modern amplitude tools include the unitarity method [68–70] which constructs loop-level scattering amplitude integrands from lower-order gauge-invariant on-shell data, as well as the double copy which relates gauge and gravity theories [71–75]. Furthermore, amplitude methods also incorporate powerful integration procedures [76], originally developed for particle-collider physics applications, such as integration by parts (IBP) [77–79], differential equations [80–85], and reverse unitarity [86–89].

Combining techniques based on scattering amplitudes with those of effective field theory (EFT), two-body effective Hamiltonians have been derived in refs. [38–40, 67] that straightforwardly determine the conservative classical dynamics of bound orbits via their equations of motion, whenever nonlocalities associated with the tail effect [90–95] are absent. Such Hamiltonians can be imported into the EOB framework [35, 41] used by LIGO for constructing gravitational-wave templates. One can alternatively obtain bound-state physical observables from the ones of hyperbolic scattering processes via appropriate analytic continuation [96–99]. Cases involving the tail effect are more subtle [100, 101].

Scattering amplitudes are the natural realm to describe the hyperbolic motion of classical objects from the asymptotic past to the asymptotic future. This idea has been implemented in the work by Kosower, Maybee, and O’Connell (KMOC) [44] whose approach allows us to extract classical observables directly from scattering amplitudes and what are essentially unitarity cuts. Alternatively, in the classical limit, appropriately defined finite parts of the scattering amplitudes can be directly connected to the scattering angle or the isotropic gauge two-body Hamiltonian [40, 96]. The scattering amplitude can also be interpreted directly in terms of the radial action [60, 102, 103]. A related but distinct approach based on the eikonal phase [104] (for more recent examples see e.g. refs. [49, 50, 105–111]) provides a natural way to extract the classical scattering angle from amplitudes. In this paper we will use a variety of these approaches to extract classical observables in both the conservative and radiative sectors.

The usefulness of the scattering amplitude framework has been demonstrated through the first construction of the conservative two-body Hamiltonian at $\mathcal{O}(G^3)$ [39, 40] (whose various aspects are confirmed in multiple studies [53–56, 58]), as well as new results at $\mathcal{O}(G^4)$ [60, 63]; see also refs. [65, 66, 112]. There have also been a variety of new results for spin [113–129], tidal effects [130–139], and waveforms [48].

In carrying out such calculations, it is useful to analyze simpler models compared to Einstein gravity that eliminate unnecessary complications. As a recent example, the authors of ref. [140] analyzed $\mathcal{N}=8$ supergravity to demonstrate the cancellation of mass singularities between conservative and radiative contributions to the classical scattering angle, leading to a complete resolution [141]. Likewise, gauge theory, especially electrodynamics, served as a toy model for gravity in the context of two-body dynamics for many decades [33, 44, 50, 99, 142]. While being a linear theory, it captures some of the technical difficulties encountered with general relativity (GR) at high orders of perturbation theory. Another reason for studying corresponding quantities in gauge theories, especially in non-abelian cases, is the double-copy relation between gauge and gravity theories [71–73].

Recently, the conservative and radiative dynamics in classical relativistic scattering was obtained by Saketh, Vines, Steinhoff, and Buonanno in scalar electrodynamics to the sixth order in the charges or the third order in the fine-structure constant [99]. This was accomplished by the direct iteration of the equations of motion. Here, we compare to these results using scattering amplitudes based approaches, finding full agreement. Using amplitude methods, we evaluate the angle including radiative effects in three distinct ways. First, we use the Kosower-Maybee-O’Connell formalism to obtain the impulse on two massive charged scalar particles scattering at large impact parameter b from which we extract the scattering angle. As an alternative, we extract the eikonal phase from the scattering amplitude which allows us to determine the scattering angle. Finally, using recent observations on the connection of the scattering amplitude in the classical limit to the radial action [60] (see also [102]), we present a simple prescription for extracting from the scattering amplitude a (generalized) radial action that determines the scattering angle, *including* radiative effects. Although the system is not conservative, we find that the scattering angle obtained by differentiating this generalized radial action agrees with the previous results. All three amplitudes-based approaches for extracting the classical scattering angle match, and agree with the classical result of ref. [99].

As previously discussed in ref. [99], in electromagnetism we encounter a mass singularity in the scattering angle, which does not cancel between potential and radiative contributions, as it does in the corresponding $\mathcal{O}(G^3)$ calculation in gravity [140, 141]. In fact, the singularity is power divergent for $m \rightarrow 0$, similar to the situation in the conservative sector of gravity at $\mathcal{O}(G^4)$ [60, 63]. From our perspective, we interpret this singularity as a breakdown of the classical massive point particle expansion which requires that the Compton wavelength $\lambda_c = \hbar/m$ is much larger than the inter-particle separation $|b|$. This leads to the hierarchy of scales $m|b| \gg \hbar$ which would be violated as we take $m \rightarrow 0$, keeping $|b|$ fixed.¹ Another interesting feature of the amplitudes based approaches is that the Abraham-Lorentz-Dirac (ALD) force in electromagnetism [143–146] and the analogous Mino, Sasaki, Tanaka, Quinn and Wald (MSTQW) force [11, 12, 147], that appears in

¹Classical scattering of massless particles still makes sense, as discussed, e.g. in the classic work of Amati, Ciafaloni, and Veneziano [105]. In this setup, one starts from scattering amplitudes of massless states. In all inequalities that define the classical high-energy scattering regime, the particle masses get replaced by energies. In contrast, in our computations, we explicitly assume massive states in various stages of the computation, most notably in the expansions in small momentum transfer $|q|/\hbar m \ll 1$.

more radiational methods [33] is automatically built in and does not require any special treatment [44].

For the conservative sector, we also extracted a two-body Hamiltonian valid through the sixth order in the charges analogous to the $\mathcal{O}(G^3)$ isotropic-gauge Hamiltonian of the gravitational case. This is obtained from the mapping between infrared-finite parts of the amplitude to the coefficients in the two-body potential [40, 96]. As for any standard Hamiltonian it can be directly applied to the bound state case.

The paper is organized as follows. In section 2 we briefly review the methods used here. Then in section 3 we evaluate the conservative contributions to the two-particle scattering through the sixth order in the charges. In section 4 we include radiative corrections to the scattering angle and impulse and also compute the radiated momentum. We give our conclusions in section 5. All our results are available in computer-readable form in the ancillary file attached to this article.

2 Review of methods

The present section briefly summarizes and reviews the main technical ingredients that are required to obtain classical scattering observables in (scalar) QED up to two-loop order ($\mathcal{O}(\alpha^3)$) where $\alpha = e^2/4\pi\hbar$ is the dimensionless fine-structure constant in units where $c = 1, \epsilon_0 = 1$), corresponding to the sixth order in the charges, from various scattering amplitude based frameworks. Readers only interested in the final results may skip this section on a first reading. The remainder of this section is structured as follows: we first review the kinematic parametrization tailored towards the classical expansion of quantum scattering amplitudes in subsection 2.1, before outlining the generalized unitarity framework to determine the amplitude integrands in subsection 2.2. In subsection 2.3, we telegraphically sketch the applicability of modern collider-physics based integration tools to compute precision-level classical observables with the help of integration-by-parts reduction to a minimal set of master integrals and their evaluation by differential equation methods. Subsection 2.4 introduces a new concept that allows us to define a radial action in the presence of soft-region radiation effects. In particular, we find an efficient computational scheme that allows us to compute the *soft radial action* by a well-motivated modification of the boundary conditions for the soft-region master integrals. Finally, in subsection 2.5, we briefly summarize the Kosower, Maybee, and O’Connell (KMOC) formalism which allows us to extract the classical electromagnetic impulse, the radiated momentum, and the classical scattering angle up to $\mathcal{O}(\alpha^3)$.

2.1 Classical limit of quantum scattering amplitudes — soft and potential region

We compute classical observables for the relativistic scattering of two point-charges, in what might be called the “post-Lorentzian” (PL) expansion. This regime is in direct correspondence to the post-Minkowskian expansion in gravity.

The relevant length scales, summarized in table 1, are the Compton wavelength $\lambda_c = \hbar/m$, related to Planck’s constant \hbar and the particle mass scale m , the typical classical

	GR	QED
quantum:	$\lambda_c \sim \frac{\hbar}{m}$	$\lambda_c \sim \frac{\hbar}{m}$
classical particle size:	$r_S \sim Gm$	$r_Q \sim \frac{e^2 q_i^2}{\hbar} \frac{\hbar}{m} = \alpha \lambda_c$
particle separation:	$ b \sim \frac{\hbar}{ q }$	$ b \sim \frac{\hbar}{ q }$

Table 1. Comparison between relevant length scales in the post-Minkowskian (PM) expansion in GR and the post-Lorentzian (PL) regime in (scalar) QED in units where $c = 1$ and the fundamental charge e is measured in units where $\epsilon_0 = 1$. The classical impact parameter b is Fourier conjugate to the momentum transfer q/\hbar in scattering amplitudes.

particle size $r_S \sim GM$ or $r_Q \sim \hbar(eq_i)^2/(4\pi\hbar m) \sim \alpha\lambda_c$ (Schwarzschild radius or classical charge radius), as well as the inter-particle separation b . The classical PM expansion corresponds to the following hierarchy of scales: $\lambda_c \ll r_S \ll |b|$, and similarly $\lambda_c \ll r_Q \ll |b|$ in the PL case. The classical limit posits that the individual particle size is much bigger than the Compton wavelength and forces us into a regime of large charges: $r_S/\lambda_c \gg 1 \leftrightarrow Gm^2/\hbar \gg 1$, or $r_Q/\lambda_c \gg 1 \leftrightarrow e^2q_i^2/\hbar \gg 1$, where q_i is the electric charge of the classical object in units of e . The large (macroscopic) charge regime makes intuitive sense from the point of view that classical physics should arise from the quantum theory in the limit of large quantum numbers. This regime seems to suggest that we are outside the traditional range of validity of perturbation theory where we would demand that $Gm^2/\hbar \ll 1$, or $e^2q_i^2/\hbar \ll 1$. This, however, is a premature conclusion, because the PM or PL regime amounts to an expansion in terms of the small ratio $r_S/|b| \ll 1$ or $r_Q/|b| \ll 1$ which leads to a well-defined perturbative expansion. For an especially nice discussion of the relevant scales in the gravitational context, see e.g. ref. [148]. In conclusion, we are left with the following hierarchy of scales $\lambda_c/b \ll r_S/|b|$, $r_Q/|b| \ll 1$.

In order to simplify our discussion, we focus on the scattering of spinless, structureless objects described by massive scalar fields. In the PL approximation, the above hierarchy of scales is converted into momentum space as follows: the impact parameter b is Fourier conjugate to the momentum transfer q/\hbar in the scattering process, $|b| \sim \hbar/|q|$. The above position space inequalities turn into $|q|/m \ll Gm|q|/\hbar$, $\alpha|q|/m \ll 1$ in gravity and QED, respectively. The masses of the scalars are very heavy and the momentum transfer $|q| \sim \hbar/|b|$ is small in the classical limit, $(-q^2) \ll m_i^2$, in complete analogy to gravitational scattering. In order to extract classical physics, we utilize special kinematic variables that facilitate the classical $\hbar \rightarrow 0$ or equivalently *soft* (small $|q|/m$) expansion² in the context of the method of regions [149]. These variables have previously appeared in e.g. Ref. [76] and are summarized in figure 1,

$$p_1 = -\left(\bar{p}_1 - \frac{q}{2}\right), \quad p_2 = -\left(\bar{p}_2 + \frac{q}{2}\right), \quad p_3 = \left(\bar{p}_2 - \frac{q}{2}\right), \quad p_4 = \left(\bar{p}_1 + \frac{q}{2}\right). \quad (2.1)$$

The new vectors \bar{p}_i are orthogonal to the momentum transfer q , $\bar{p}_i \cdot q = 0$, which directly follows from the on-shell conditions $p_1^2 = p_4^2 = m_1^2$ and $p_2^2 = p_3^2 = m_2^2$. For later convenience,

²From now on, we work in natural units and set $\hbar = 1$ unless stated otherwise.

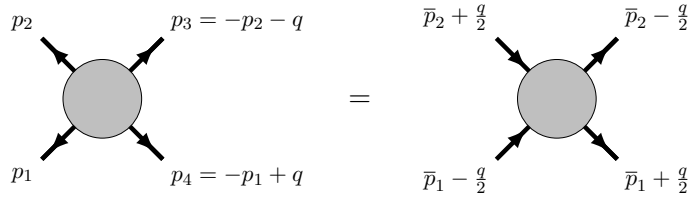


Figure 1. Parametrization of external kinematics.

we also introduce ‘soft-masses’ \bar{m}_i defined by

$$\bar{m}_i^2 = \bar{p}_i^2 = m_i^2 - \frac{q^2}{4} \quad \rightarrow \quad \bar{m}_i = m_i + \frac{(-q^2)}{8m_i} + \mathcal{O}(q^4). \quad (2.2)$$

Notably, in the specialized barred variables, $s = (\bar{p}_1 + \bar{p}_2)^2 = (p_1 + p_2)^2$ the physical scattering region $s > (m_1 + m_2)^2$, $q^2 < 0$ remains the same. Following earlier conventions [76], we define the soft four-velocities of the two black holes $u_i^\mu = \bar{p}_i^\mu / |\bar{p}_i|$, such that $u_i^2 = 1$, and

$$y \equiv u_1 \cdot u_2 = \frac{1 + x^2}{2x} = \sigma - (-q^2) \frac{(m_1^2 + m_2^2)\sigma + 2m_1m_2}{8m_1^2m_2^2} + \mathcal{O}(q^4). \quad (2.3)$$

For physical scattering in the s -channel we have $y > 1$. Often, it will prove advantageous to change variables to x in the range $0 < x < 1$ in order to rationalize the naturally appearing square-root $\sqrt{y^2 - 1} = \frac{1-x^2}{2x}$.

Note that the soft velocities u_i coincide with the classical four velocities of the massive scalars only up to corrections of $\mathcal{O}(q)$. The KMOC setup directly targets physical observables where this difference is immaterial. However, for the eikonal computations, the $\mathcal{O}(q)$ corrections do matter and one has to carefully track them. In the classical limit (without restricting to the conservative sector), we are interested in the soft expansion of loop amplitudes with the hierarchy of scales given by $|\ell| \sim |q| \ll |\bar{p}_i|, m, \sqrt{s}$. Here, ℓ schematically represents arbitrary combinations of photon momenta of the form $(\ell_1, \ell_2, \ell_1 \pm \ell_2, \dots)$ and typical photon propagators take the form $\frac{1}{\ell^2}, \frac{1}{(\ell-q)^2}$. These have a homogeneous $|q|$ -scaling and do not require any further expansions. Distinctly, matter propagators do have a non-trivial $|q|$ expansion expressed via dimensionless velocity variables u_i

$$\frac{1}{(\ell - p_i)^2 - m_i^2} = \frac{1}{\ell^2 - 2\ell \cdot p_i} = \frac{1}{2u_i \cdot \ell} \frac{1}{m_i} - \frac{\ell^2 \mp \ell \cdot q}{(2u_i \cdot \ell)^2} \frac{1}{m_i^2} + \dots \quad (2.4)$$

Each order in the expansion is homogeneous in $|q|$ and the mass dependence factorizes. The matter propagators effectively “eikonalize” and the soft expansion to higher orders in $|q|$ can lead to raised propagator powers.

To focus on conservative dynamics one would perform a further expansion where the temporal part of any photon line is suppressed by an additional power of the formally small velocity v , related to $y \approx \sigma = \frac{1}{\sqrt{1-v^2}}$ to signal instantaneous interactions. These *potential region* expansions have been described in great detail elsewhere [39, 40, 76] and we refrain from repeating them here for the sake of brevity.

2.2 Generalized unitarity and scalar QED scattering amplitudes up to $\mathcal{O}(\alpha^3)$

As we are going to review in the following subsections, a number of novel approaches to the classical two-body problem in gravity and electromagnetism involve the (classical limit of) quantum scattering amplitudes. These enter either in the EFT matching calculation to a classical two-body potential, in the eikonal approach to classical scattering, or in the KMOC framework that expresses classical physical observables (e.g. the impulse or the radiate momentum) in terms of scattering amplitudes and weighted cross-section-like objects. Therefore, it is crucial to have at our disposal compact expressions for the relevant (classical parts) of the higher-loop scattering amplitudes in the theories under consideration. Recent years have seen enormous advances in our ability to obtain analytic results for quantum scattering amplitudes via modern on-shell methods. On one hand, this progress enhanced our ability to compute phenomenologically relevant collider physics processes in quantum chromodynamics (QCD) and the Standard Model. On the other hand, in simplified toy theories such as maximally supersymmetric Yang-Mills theory or in supersymmetric gravity theories, similar computations were crucial to shed light on a number of impressive theoretical insights into the deeper structures of quantum field theory. A chief ingredient in many of these calculations is an efficient way to obtain a scattering amplitude *integrand*, i.e. an expression of the amplitude before loop integration. Generalized unitarity [68–70] is based on the factorization of amplitudes into simpler gauge-invariant on-shell building blocks which allows to export the simplicity of tree-amplitudes to loop-calculations. In the context of classical gravitational dynamics, these methods have been recently used [47] to obtain the radiated momentum and the impulse at $\mathcal{O}(G^3)$ in general relativity from the KMOC setup and from eikonal considerations [148]. Since these methods have been comprehensively documented elsewhere in the context of general relativity [39, 40, 47, 76], we are only giving a telegraphic account of the main ingredients of our QED calculation.

2.2.1 Tree-level amplitudes in scalar QED

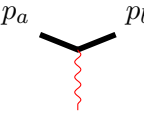
The main building blocks in the derivation of loop integrands via generalized unitarity are on-shell tree-level amplitudes out of which unitarity cuts are built. Later, these products of tree-level amplitudes are compared to the unitarity cuts of a putative ansatz of Feynman-like loop integrals in order to fix the free coefficients in the ansatz by solving a linear system of equations. We are interested in the scattering of two massive charged scalars in scalar QED that have charges $e q_{1,2}$ and masses $m_{1,2}$, respectively and interact via the exchange of U(1) gauge bosons, i.e. photons. The Lagrangian for the system is

$$\mathcal{L} = -\frac{1}{4}F_{\mu\nu}F^{\mu\nu} + \sum_{i=1}^2 \left[(D_\mu \phi_i)^\dagger (D^\mu \phi_i) - m_i^2 \phi_i^\dagger \phi_i \right], \quad (2.5)$$

where the covariant derivative $D^\mu = \partial^\mu - i e q_i A^\mu$ contains the photon field $A^\mu(x)$ and the appropriate electric charge q_i (in multiples of the fundamental charge³ e) of the scalar ϕ_i . The U(1) field strength is $F_{\mu\nu} = \partial_\mu A_\nu - \partial_\nu A_\mu$.

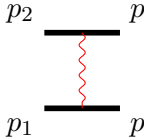
³In the following, we often trade the square of elementary charges for the coupling constant $\alpha = e^2/(4\pi)$.

The basic input is the three-point coupling between the scalars and a photon in an all-outgoing convention for the particle momenta



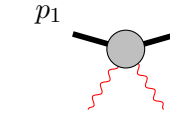
$$= -i e q_i (p_a - p_b)^\mu, \quad (2.6)$$

from which we can build the tree-level scattering amplitude between the two charged scalars due to photon exchange



$$\mathcal{A}_4^{\text{tree}}(p_1, p_2, p_3, p_4) = -\frac{4e^2 q_1 q_2 \bar{m}_1 \bar{m}_2 y}{-q^2}, \quad (2.7)$$

written in terms of the soft-kinematics of eq. (2.1). (Note that q_1 and q_2 are charges in units of e while q is the momentum transfer.) For higher-order calculations, we also require the Compton amplitude for the tree-level scattering of two scalars with two photons



$$= \frac{-2e^2 q_i^2}{(2p_1 \cdot p_2)(2p_1 \cdot p_3)} \left[2p_1 \cdot F_2 \cdot F_3 \cdot p_4 + 2p_1 \cdot F_3 \cdot F_2 \cdot p_4 + \frac{1}{2}(p_1 + p_4)^2 F_2 \cdot F_3 \right]$$

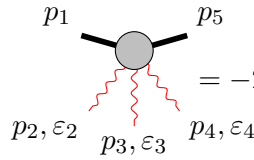
$$= -2e^2 q_i^2 \left[\varepsilon_2 \cdot \varepsilon_3 - \frac{\varepsilon_2 \cdot p_1 (\varepsilon_3 \cdot p_1 + \varepsilon_3 \cdot p_2)}{p_1 \cdot p_2} - \frac{\varepsilon_3 \cdot p_1 (\varepsilon_2 \cdot p_1 + \varepsilon_2 \cdot p_2)}{p_1 \cdot p_3} \right], \quad (2.8)$$

where we have introduced the linearized field-strengths $F_i^{\mu\nu} = \varepsilon_i^\mu p_i^\nu - \varepsilon_i^\nu p_i^\mu$. From the first line of eq. (2.8) it is clear that we have expressed the amplitude in terms of gauge-invariant building blocks that manifestly vanish when $\varepsilon_i \rightarrow p_i$, so that physical state sums that appear in the cut sewing procedure of generalized unitarity can be performed by the simple substitution (see the discussion in ref. [150])

$$\sum_\lambda \varepsilon_{i,\lambda}^{*\mu}(k) \varepsilon_{i,\lambda}^\nu(-k) \rightarrow \eta^{\mu\nu}, \quad (2.9)$$

where λ denotes the physical polarizations. To get to the compact expression on the second line of eq. (2.8), we have used momentum conservation to eliminate p_4 and the transversality condition $\varepsilon_i \cdot p_i = 0$ of the polarization vectors.

For the two-loop computation, we also require the amplitude between three photons and two massive scalars



$$= -2ie^3 q_i^3 \left[\frac{(\varepsilon_3 \cdot \varepsilon_4)(p_1 \cdot F_2 \cdot p_5)}{(p_1 \cdot p_2)(p_2 \cdot p_5)} - \frac{\varepsilon_2 \cdot p_1}{p_1 \cdot p_2} \left[\frac{(\varepsilon_3 \cdot p_5) \varepsilon_4 \cdot (p_3 + p_5)}{p_3 \cdot p_5} + \frac{(\varepsilon_4 \cdot p_5) \varepsilon_3 \cdot (p_4 + p_5)}{p_4 \cdot p_5} \right] + (2 \leftrightarrow 3) + (2 \leftrightarrow 4) \right]. \quad (2.10)$$

One can check that the representation of the amplitude satisfies generalized gauge invariance [150] for each of the photon lines. This property is defined to be that longitudinal states automatically decouple without the need to impose physical state conditions on other legs. The net effect is that state sums simplify as described in eq. (2.9).

2.2.2 One-loop integrand in scalar QED

Equipped with the tree-level building blocks, we follow the generalized-unitarity framework [68–70] to write an ansatz of Feynman-like graphs with associated numerators dictated by the power-counting of scalar QED. At one loop, we can write the full integrand in terms of box, triangle, and bubble topologies. However, sometimes it is convenient to re-absorb contributions from topologies with fewer propagators (‘contact terms’) into the definition of the box numerator by multiplying the contact terms by appropriate powers of inverse propagators D_i .

$$\begin{array}{c}
 p_2 \quad \overline{D_2} \quad p_3 \\
 \overline{D_3} \quad \square \quad \overline{D_4} \\
 p_1 \quad \overline{D_1} \quad p_4
 \end{array}
 = \int \frac{d^D \ell}{(2\pi)^D} \frac{1}{D_1 D_2 D_3 D_4}
 \tag{2.11}$$

where the inverse propagators D_i are

$$D_1 = (\ell - p_1)^2 - m_1^2, \quad D_2 = (\ell + p_2)^2 - m_2^2, \quad D_3 = \ell^2, \quad D_4 = (\ell - q)^2.
 \tag{2.12}$$

We employ the graphical notation in which thin lines denote massless propagators and thick lines denote the propagators of the massive particles. (We do not graphically distinguish particles of mass m_1 and m_2 that are always associated to the external momenta p_1, p_4 and p_2, p_3 , respectively.) As has been advocated in e.g. ref. [151], it is advantageous to directly express the numerator ansatz in terms of a basis of inverse propagators and irreducible elements (absent at one-loop). The power-counting of scalar QED dictates, that the numerator of the box integral should have a mass-scaling like $(p_i \cdot p_j)^2$. To build the ansatz, we write the numerator in terms of the following external Lorentz-products

$$\{p_1^2, p_2^2, s, -q^2\} \cup \{D_1, D_2, D_3, D_4\}.
 \tag{2.13}$$

From the power-counting of QED discussed above, we know that our numerator ansatz is quadratic in the variables of eq. (2.13), so that

$$n_{\text{box}}^{\text{ansatz}} = a_1(p_1^2)^2 + \dots + a_{63}D_3D_4 + a_{64}D_4^2.
 \tag{2.14}$$

Every numerator basis element that is proportional to one of the inverse propagators D_i corresponds to a contact term, so that we do not have to list these topologies separately. In a first step, we impose diagram symmetries of the scalar graph in eq. (2.11) which reduces the number of unknown coefficients a_i and ensures that we only have to determine the numerator for this single graph.

In order to find the desired integrand, we subsequently compare the cut of the ansatz against the field theory result as determined by the product of tree-level amplitudes

summed over the exchanged on-shell states that can cross the cut. Since we are interested in the classical, long-range interactions between the heavy scalar particles mediated by photon exchange, we never need to consider contact (i.e. short distance) interactions between the scalars. In order to obtain the relevant classical and quantum terms (required for the two-loop eikonal calculation in sections 3.2, 4.2) of the one-loop amplitude, it suffices to match the two-particle bubble-cut


(2.15)

Matching the above field theory cut (i.e. the product of two Compton amplitudes of eq. (2.8)) with our basis ansatz requires relabeling the basic box integrand of eq. (2.11) with the associated numerator (2.14). Solving the cut equations and dropping all terms proportional to inverse propagators that correspond to pinches of photon lines (which would correspond to short-distance contact interactions that are irrelevant for the classical physics of interest), we find

$$n_{\text{box}} = -4e^4 q_1^2 q_2^2 \left(4(p_1 \cdot p_2)^2 - p_2^2 D_1 - p_1^2 D_2 - (D_1^2 + D_2^2) + \frac{1}{4}(D_s - 2)D_1 D_2 \right). \quad (2.16)$$

The terms proportional to $D_1 D_2$ correspond to a bubble integral that is only relevant for the quantum subtraction for the two-loop eikonal analysis. The triangle topologies are included through the numerators proportional to D_1 and D_2 , respectively. The result (2.16) is written in terms of the state-counting parameter $D_s = \eta^\mu{}_\mu$ and we will work in the scheme where we set $D_s = 4$ and write the one-loop amplitude as a sum of a box and cross-box,

$$\mathcal{A}_4^{(1)}(p_1, p_2, p_3, p_4) = n_{\text{box}} \left[\begin{array}{c} p_2 \quad p_3 \\ \text{---} \quad \text{---} \\ | \quad | \\ \text{---} \quad \text{---} \\ p_1 \quad p_4 \end{array} \right] + n_{\text{x-box}} \left[\begin{array}{c} p_2 \quad p_3 \\ \text{---} \quad \text{---} \\ \diagdown \quad \diagup \\ \text{---} \quad \text{---} \\ p_1 \quad p_4 \end{array} \right], \quad (2.17)$$

where the numerator for the second box, $n_{\text{x-box}}$, is obtained from eq. (2.16) by crossing $p_1 \leftrightarrow p_4$ and (the immaterial) $q_1 \rightarrow -q_1$.

2.2.3 Two-loop integrand in scalar QED

At two-loops, the cut construction proceeds in a fashion similar to the previous one-loop analysis. We start from the relevant graphs with cubic vertices, summarized in figure 2 and write down a numerator ansatz for each diagram consistent with QED power counting: each trivalent vertex is associated with one power of momentum in the numerator. We then impose the diagram symmetries of the graphs on the respective numerator ansatz. To determine the pieces of the scalar QED two-loop amplitudes relevant for classical physics, both in the eikonal and KMOC approach, we fix the numerators by matching against the spanning sets of cuts depicted in figure 3 built out of products of the tree-level amplitudes from section 2.2.1.

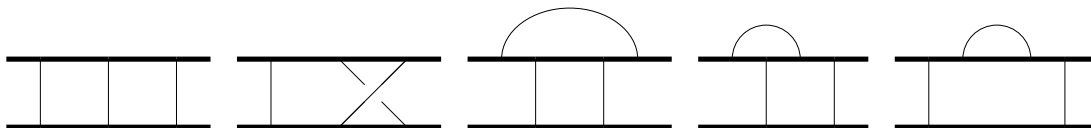


Figure 2. Diagrams with cubic vertices relevant for classical $\mathcal{O}(\alpha^3)$ observables in scalar QED. The first two graphs appear in the conservative sector and the three “mushroom” graphs are only relevant for radiative effects. The diagrams split into different gauge-invariant subsectors. The III and IX graphs (corresponding to the first two diagrams) are proportional to $q_1^3 q_2^3$, whereas the mushroom graphs are proportional to $q_1^2 q_2^4$ (and $q_1^4 q_2^2$ for the flipped graphs not explicitly drawn).

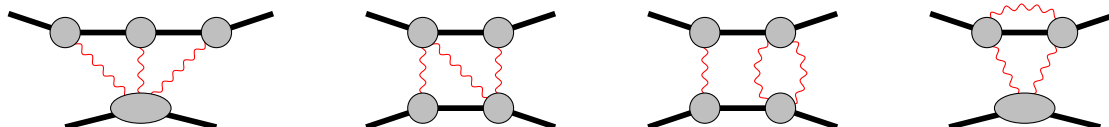


Figure 3. Spanning set of unitarity cuts relevant for the classical dynamics at $\mathcal{O}(\alpha^3)$.

2.3 Soft and potential region expansion, IBP, and differential equations

With the relevant one- and two-loop integrands at hand, we directly follow similar computations that have been performed in the gravitational setting [39, 40, 46, 47, 76]. In particular, we expand the scalar QED integrands of subsection 2.2 in either the soft or potential region. We take advantage of the technology developed in refs. [47, 76] and import the explicit values of all soft master integrals supplied in the ancillary files of ref. [47] (for an alternative computation of the soft master integrals, see ref. [148]). We will not review these steps in any detail and refer the interested reader to the original references. Briefly, there are two main steps involved in order to obtain integrated results. The first is to start from the initial integrands and expand them in small $|q|$ which leaves graviton propagators unaffected and linearizes (eikonalizes) all matter propagators. This step is related to the kinematic discussion in subsection 2.1. To obtain conservative physics (i.e. the potential region in the language of the method of regions [149]), one further expands the propagators in a formal small velocity parameter v , where the graviton energy component is suppressed by an extra factor of v compared to the spatial components. This signals instantaneous interactions in the Fourier-conjugate time domain. In either case, upon expanding the integrand in the desired kinematic region of interest, one subsequently reduces all resulting integrals to a basic set of so-called master integrals. One can then solve for the values of the remaining master integrals using modern differential equation methods [80–85]. For the KMOC setup, besides the virtual two-loop integrals, one also needs to have access to certain cut-integrals whose computation was significantly simplified using reverse unitarity [86–88]—a well-known tool from collider physics computations (see e.g. ref. [89]). In this work, we leverage the fact that all relevant integrals have been computed to the order required for our work and we essentially re-use the integration pipeline that already has been successfully implemented for GR both in the soft [46, 47] and potential region [39, 40, 76].

2.4 Soft radial action and master integral subtraction of classically divergent terms

In the discussion so far, we mainly focused on the computation of scattering amplitudes in the so-called *soft region* where we only assume that the momentum transfer $-q^2 \ll m_i^2$, s is much smaller than the masses or the energy of the scattering process. As we will explain in most of the remainder of our work, these amplitudes then enter either the eikonal formalism or the KMOC framework in order to extract the relevant classical observables from the scattering amplitudes (or certain combinations of scattering amplitudes). Crucially, inherent in both the eikonal or the KMOC formalism is the fact that amplitudes not only have classical contributions but, at higher orders in perturbation theory, also involve classically divergent (‘super-classical’) terms that are more singular and have to cancel for classically well-defined observables.⁴ In light of this discussion, one might wonder, whether or not there exists a formalism that directly targets the classical terms directly, without the need to compute the classically divergent terms directly and avoid problems at higher perturbative order of the form \hbar/\hbar where the classically divergent terms interfere with quantum contributions to yield a naively classical result. In the conservative sector, [60] advocated for an EFT based approach with a particular subtraction scheme of classical iterations that allowed the definition and computation of the *radial action* I_r directly from the relation (eq. (2) of ref. [60])

$$i\mathcal{A}(\mathbf{q}) = \int_J \left[e^{iI_r(J)} - 1 \right], \tag{2.18}$$

which looks very similar to the eikonal exponentiation, but differs in important details [60].

As is well-known from classical physics, see e.g. ref. [152], the radial action is an important quantity, associated with the classical Hamilton-Jacobi equation for the system, from which to extract relevant classical observables. See e.g. recent work in the probe-limit [103]. Subsequently, the authors of ref. [102] argued for a related exponential representation of the S-matrix, $S = e^{i\hat{N}}$, where one calculates its phase, \hat{N} , from which one can extract classical observables (including radiation) due to a relation to the WKB approximation. This has been assembled into a computational framework in ref. [153] where the radial action has been tied to certain *velocity cuts* (see also ref. [154] for related work).

Similarly to the eikonal approach, the radial action $I_r(J)$ (and also the phase of the S-matrix \hat{N}) has a perturbative expansion $I_r(J) = I_r^{(0)}(J) + I_r^{(1)}(J) + I_r^{(2)}(J) + \dots$ which leads to classical iterations from expanding the exponential to higher orders in the small coupling constant. In this section, we describe an approach to calculate the classical radial action at a given loop order $I_r^{(L)}(J)$ without the need of explicit classically divergent subtractions. Our new setup is closest in philosophy to that of ref. [60]. In particular, we are going to find a prescription that is implemented at the level of boundary conditions for soft master integrals which manifestly eliminates classically divergent contributions, and allows us to

⁴Similar statements also hold in the EFT matching approach for the conservative two-body problem where classically divergent terms correspond to iterations of lower-order potentials, see e.g. ref. [60] and references therein.



Figure 4. Master integral topologies related to iteration of radial action or EFT potential, responsible for classically divergent terms in the amplitude. The IX diagram corresponding to the second one in figure 2 does not appear since it is not divergent in the potential region, so receives no subtraction in a conservative calculation. The subtraction in the soft region is designed to be identical to the subtraction in the potential region — this works as long as we restrict to the real part where the only divergences comes from $\mathcal{A}_{\text{tree}}^3$.

define a soft radial action. By explicit calculation, we show that our prescription works up to two-loop order. Its study to higher orders in perturbation theory is an interesting open problem left to future work.

Formally, the perturbative expansion of eq. (2.18) to a given loop-order L still entails the subtraction of nontrivial exponentiation terms involving two or more lower-order *iterations* $I_r^{(L' < L)}$ to isolate $I_r^{(L)}$ itself. The aforementioned reference [60] writes such iterations as $(D-1)$ -dimensional integrals with linearized propagators. Meanwhile, the boundary conditions for soft master integrals near the static limit, when considering only the potential region, are also given by $(D-1)$ -dimensional integrals where the “divergent” part involves linearized propagators [76]. Therefore, our strategy is to drop integrals with linearized propagators from the boundary conditions and then solve the differential equations for the soft integrals subject to the modified “finite” boundary conditions.

The set of diagram topologies for master integrals related to the above “iterations” is shown in figure 4. It turns out that only the first graph in figure 4, called the III diagram, is relevant for the classically divergent terms in the real part of the two-loop amplitude. In the notation of eq. (4.70) of [76], the top-level soft master integral for the III diagram is

$$f_{\text{III},7} = \epsilon^4 (y^2 - 1) (-q^2) G_{1,1,1,1,1,1,1,0,0}, \quad (2.19)$$

where $G_{1,1,1,1,1,1,1,0,0}$ is the scalar double-box integral with a unit numerator, multiplied by additional prefactors are included. In the Euclidean region we have $-1 < x < 0$, and $y = (1 + x^2)/(2x) < -1$, with the value of the master integral given in ref. [76] as

$$f_{\text{III},7} = -\frac{1}{2}\epsilon^2 \log^2(-x) + \frac{1}{12}\epsilon^3 [-24\text{Li}_3(x) - 24\text{Li}_3(-x) + 12\text{Li}_2(x) \log(-x) + 12\text{Li}_2(-x) \log(-x) + 2\log^3(-x) + \pi^2 \log(-x) + 6\zeta_3] + \mathcal{O}(\epsilon^4). \quad (2.20)$$

By analytic continuation, the value of integral in the Lorentzian region $0 < x < 1$, $y > 1$ is obtained from the above formula with an infinitesimal positive imaginary part given to y , or an infinitesimal negative imaginary part given to x ,

$$f_{\text{III},7} = -\frac{1}{2}\epsilon^2 [\log(x) + i\pi]^2 + \mathcal{O}(\epsilon^3), \quad (2.21)$$

where we omitted the analytic continuation result at $\mathcal{O}(\epsilon^3)$ which is needed for calculating the amplitude but not relevant for the discussion here.

When evaluated in the potential region, the integral cannot be analytically continued between positive and negative values of x , and we directly give the value of the integral for the Lorentzian region $0 < x < 1$, $y = (1+x^2)/(2x) > 1$,

$$f_{\text{III},7}^{(p)} = \frac{\epsilon^2 \pi^2}{2} + 0 \cdot \epsilon^3 + \mathcal{O}(\epsilon^4). \quad (2.22)$$

Compared with eq. (2.21), in the $\mathcal{O}(\epsilon^2)$ term only the π^2 part survives, and the $\mathcal{O}(\epsilon^3)$ term has become genuinely zero, and not an omission.

There are 7 pure master integrals for the soft-expanded III diagram in the even-in- $|q|$ sector. In the potential region, the boundary condition near the static limit $y = 1$ is given in terms of $(3 - 2\epsilon)$ -dimensional integrals in eqs. (A.9)-(A.11) of ref. [76]. In particular, for the top-level master integral near the static limit,

$$f_{\text{III},7}^{(p)}|_{y=1} = \pi \epsilon^4 (-q^2) \int \frac{d^{D-1} \ell_1 d^{D-1} \ell_2 (e^{\gamma_E \epsilon})^2}{(i\pi^{(D-1)/2})^2 \ell_1^2 \ell_2^2 (\ell_1 + \ell_2 - \mathbf{q})^2 (2\ell_1^z)(-2\ell_2^z)}, \quad (2.23)$$

which is precisely of the form of a $(D - 1)$ -dimensional integral involving linearized propagators. The superscript (p) in the equation above indicates that only the potential region is considered. Now we implement a subtraction scheme similar to the 4PM potential-region calculation, by dropping $(3 - 2\epsilon)$ -dimensional integrals involving linearized propagators arising from iterations of lower-loop potentials. This is equivalent to keeping eqs. (A.9) and (A.10) in the reference while changing the r.h.s. of eq. (A.11), reproduced in eq. (2.23), to zero. Solving differential equations with the altered boundary conditions, eq. (2.22) becomes

$$f_{\text{III},7}^{(p),\text{subtracted}} = 0 \cdot \epsilon^2 + 0 \cdot \epsilon^3 + \mathcal{O}(\epsilon^4), \quad (2.24)$$

i.e. vanishes until $\mathcal{O}(\epsilon^4)$, which is beyond the order of ϵ needed in the classical calculation.

The boundary values for the master integrals in the soft region are decomposed into the sum of their values in the potential region and their soft-region corrections. We perform the same subtraction for the potential-region part, while keeping the soft-region corrections unchanged. Since the solutions to the homogeneous system of differential equations have multi-linear dependence on the boundary conditions, we have

$$f_{\text{III},7}^{\text{subtracted}} = f_{\text{III},7} + \left(f_{\text{III},7}^{(p),\text{subtracted}} - f_{\text{III},7}^{(p)} \right). \quad (2.25)$$

Explicitly,

$$f_{\text{III},7}^{\text{subtracted}} = -\frac{1}{2} \epsilon^2 \left[\log(x)^2 + 2i\pi \log(x) \right] + \mathcal{O}(\epsilon^3), \quad (2.26)$$

where in the $\mathcal{O}(\epsilon^2)$ term, the π^2 part has been removed, and the omitted $\mathcal{O}(\epsilon^3)$ term (also needed for assembling the amplitude) is completely unchanged.

If we calculate the two-loop amplitude in the soft expansion using the subtracted value eq. (2.26) for the top-level III master integral and unsubtracted original results for all other master integrals, the real part of the result directly gives the radial action after Fourier transform.

2.5 KMOC framework for classical conservative and radiative observables

In this part of our review, we schematically recall aspects of the KMOC framework [44] as presented in ref. [47]. We only introduce the relevant final formulae. For further details, the interested reader is encouraged to consult refs. [44] or [47] directly.

In the KMOC [44] approach one first sets up a quantum mechanical Gedanken experiment for the scattering of two wavepackets representing massive particles from which the classical limit is carefully taken in order to extract the classical observables of interest. In the quantum setup, we can measure the change of some observable ΔO (corresponding to some quantum operator \mathbb{O}) following the time-evolution of states from the asymptotic past to the asymptotic future. In the asymptotic past, the wavepackets are represented by $|\text{in}\rangle$, an *in* quantum state constructed from the superposition of two-particle momentum eigenstates $|p_1, p_2\rangle_{\text{in}}$ with wavefunctions $\phi_i(p_i)$. For the case of interest to us, these states are well separated by an impact parameter b^μ ,⁵

$$|\text{in}\rangle = \int d\Phi_2(p_1, p_2) \phi_1(p_1)\phi_2(p_2)e^{ib \cdot p_1/\hbar} |p_1, p_2\rangle_{\text{in}}. \tag{2.27}$$

Such an *in* state will evolve to an *out* state in the asymptotic future, $|\text{out}\rangle$, that might contain additional particles created during the interaction. ΔO is obtained by evaluating the difference of the expectation value of \mathbb{O} between *in* and *out* states

$$\Delta O = \langle \text{out} | \mathbb{O} | \text{out} \rangle - \langle \text{in} | \mathbb{O} | \text{in} \rangle. \tag{2.28}$$

In quantum mechanics, the *out* states are related to the *in* states by the time evolution operator, i.e. the S-matrix: $|\text{out}\rangle = S|\text{in}\rangle$ and we can write

$$\Delta O = i \int d\Phi_4(p_1, \dots, p_4) \phi_1(p_1)\phi_2(p_2)\phi_2^*(p_3)\phi_1^*(p_4) \hat{\delta}^{(D)}(\sum_i p_i) e^{ib \cdot (p_1+p_4)/\hbar} \mathcal{I}_O, \tag{2.29}$$

where we follow the same conventions as ref. [47] for the phase-space $d\Phi_n$ and $\hat{\delta}$ factors. The kernel \mathcal{I}_O is related to the matrix elements via

$$\tilde{\mathcal{I}}_O \equiv \hat{\delta}^{(D)}(\sum p_i) \mathcal{I}_O = -i \langle p_4, p_3 | S^\dagger[\mathbb{O}, S] | p_1, p_2 \rangle. \tag{2.30}$$

To arrive at this expression, we have used the unitarity of the S-matrix, $S^\dagger S = 1$. Following [44], $\tilde{\mathcal{I}}_O$ can be related to scattering amplitudes by writing $S = 1 + iT$ such that

$$\tilde{\mathcal{I}}_O = \tilde{\mathcal{I}}_{O,v} + \tilde{\mathcal{I}}_{O,r} = \langle p_4, p_3 | [\mathbb{O}, T] | p_1, p_2 \rangle - i \langle p_4, p_3 | T^\dagger[\mathbb{O}, T] | p_1, p_2 \rangle. \tag{2.31}$$

We conveniently separated the kernel $\tilde{\mathcal{I}}_O$ into two contributions $\tilde{\mathcal{I}}_{O,v}$ and $\tilde{\mathcal{I}}_{O,r}$, that we preemptively call *virtual* and *real*, respectively. This nomenclature becomes apparent when one evaluates the expectation values: the *virtual* part of the result is

$$\mathcal{I}_{O,v} = \Delta \mathbb{O} [\mathcal{A}(p_1, p_2, p_3, p_4)] = \Delta \mathbb{O} \left[\begin{array}{c} p_2 \quad p_3 \\ \diagdown \quad \diagup \\ \text{---} \circ \text{---} \text{---} \text{---} \\ \diagup \quad \diagdown \\ p_1 \quad p_4 \end{array} \right], \tag{2.32}$$

⁵The impact parameter b^μ is distinct from the eikonal impact parameter b_e that will appear later.

quantum momentum operator \mathbb{P}_i , which is measured asymptotically far from the collision region as follows

$$\Delta p_1^\mu = \langle \text{in} | S^\dagger \mathbb{P}_1^\mu S | \text{in} \rangle - \langle \text{in} | \mathbb{P}_1^\mu | \text{in} \rangle. \quad (2.38)$$

As summarized above, in the classical limit, this is simply a Fourier transform of the impulse kernel $\mathcal{I}_{p_1}^\mu$ from momentum transfer q to impact-parameter space b

$$\Delta p_1^\mu = i \int \hat{d}^D q \hat{\delta}(-2p_1 \cdot q) \hat{\delta}(2p_2 \cdot q) e^{ib \cdot q} \mathcal{I}_{p_1}^\mu, \quad (2.39)$$

which is separated into virtual and real contributions, given in terms of the amplitude as

$$\mathcal{I}_{p_1, v} = q^\mu \text{ (diagram: circle } A \text{ with } p_1, p_2, p_3, p_4 \text{)} , \quad \mathcal{I}_{p_1, r} = -i \sum_X \int d\tilde{\Phi}_{2+|X|} \ell_1^\mu \text{ (diagram: } A \text{ and } A^* \text{ with } p_1, p_2, p_3, p_4 \text{ and } \ell_X \text{)} , \quad (2.40)$$

where the numerator insertions q^μ and ℓ_1 arise from the measurement function $\Delta \mathbb{P}_1^\mu$ acting on the respective amplitudes, which extracts the momentum change of particle 1. Note that relative to eq. (2.33), we have changed variables in the real contribution by shifting the massive intermediate momenta $r_i = -p_i + \ell_i$, so that all ℓ_i are small, $\mathcal{O}(\hbar)$, in the classical expansion. The impulse on particle 2 can be obtained by simple relabelling.

In the following, we often decompose the total impulse into its transverse, Δp_\perp , and longitudinal, Δp_u , components

$$\Delta p^\mu = \Delta p_\perp^\mu + \Delta p_u^\mu, \quad (2.41)$$

where $u_i \cdot \Delta p_\perp = 0$ and $q \cdot \Delta p_u = 0$. The respective kernels get decomposed in a similar fashion

$$\mathcal{I}_{p_1}^\mu = \mathcal{I}_\perp q^\mu + \sum_{i=1,2} \mathcal{I}_{u_i} \check{u}_i^\mu. \quad (2.42)$$

We define *dual* four-velocities,

$$\check{u}_1^\mu = \frac{y u_2^\mu - u_1^\mu}{y^2 - 1}, \quad \check{u}_2^\mu = \frac{y u_1^\mu - u_2^\mu}{y^2 - 1}, \quad (2.43)$$

which satisfy $u_i \cdot \check{u}_j = \delta_{ij}$ and remain orthogonal to the momentum transfer q . Decomposing the loop momentum dependent impulse numerator

$$\ell_1^\mu = \frac{\ell_1 \cdot q}{q^2} q^\mu + (\ell_1 \cdot u_1) \check{u}_1^\mu + (\ell_1 \cdot u_2) \check{u}_2^\mu, \quad (2.44)$$

exposes that only the transverse part of the impulse has a *virtual* contribution

$$\mathcal{I}_\perp = \text{ (diagram: circle } A \text{ with } p_1, p_2, p_3, p_4 \text{)} - i \sum_X \int d\tilde{\Phi}_{2+|X|} \frac{\ell_1 \cdot q}{q^2} \text{ (diagram: } A \text{ and } A^* \text{ with } p_1, p_2, p_3, p_4 \text{ and } \ell_X \text{)} , \quad (2.45)$$

whereas the longitudinal part *only* receives contributions from the unitarity cut terms

$$\mathcal{I}_{u_i} = -i \sum_X \int d\tilde{\Phi}_{2+|X|} \ell_1 \cdot u_i \quad \begin{array}{c} p_2 \qquad \ell_2 - p_2 \qquad p_3 \\ \diagdown \quad \quad \diagup \\ \text{---} \text{---} \text{---} \\ \diagup \quad \quad \diagdown \\ p_1 \qquad \ell_1 - p_1 \qquad p_4 \end{array} \quad (2.46)$$

Loop amplitudes generically have real and imaginary parts, so one might wonder how all classical observables end up real-valued, and how various terms in the KMOC setup combine to serve this purpose. Keeping track of factors of ‘i’, it turns out that the transverse KMOC kernels need to be purely real to yield a real result after the final Fourier transform (eq. (2.34)), whereas the longitudinal kernels are purely imaginary. The reality properties of various quantities has been argued abstractly in terms of unitarity cutting rules in ref. [47] that later appeared in a slightly different context in ref. [102]. Indeed, it will serve as a nontrivial check of our computation, that all imaginary contributions to the classical observables cancel.

2.5.2 Radiated momentum

Another observable of interest is the total radiated momentum ΔR^μ carried away in the form of electromagnetic waves during the scattering of two heavy charged objects. This observable is defined by measuring the momentum operator \mathbb{R}^μ of the emitted *messenger particles*, here photons. As explained in ref. [44], this observable only receives *real* contributions and its respective kernel is

$$\mathcal{I}_{R,r}^\mu = -i \sum_X \int d\tilde{\Phi}_{2+X} \ell_X^\mu \quad \begin{array}{c} p_2 \qquad \ell_2 - p_2 \qquad p_3 \\ \diagdown \quad \quad \diagup \\ \text{---} \text{---} \text{---} \\ \diagup \quad \quad \diagdown \\ p_1 \qquad \ell_1 - p_1 \qquad p_4 \end{array} \quad (2.47)$$

Like eqs. (2.39) and (2.40), eq. (2.47) is valid beyond perturbation theory, however, for explicit calculations we expand it perturbatively in α . The first contribution to ΔR^μ (obtained from eq. (2.47) by performing the Fourier transform to impact-parameter space (2.34)) arises at $\mathcal{O}(\alpha^3)$. This can be understood from the fact that Bremsstrahlung of finite energy photons only arises once one heavy charged particle is slightly deflected due to its electromagnetic interaction with the other massive charged object.

The impulse and radiated momentum are not completely independent observables. As already pointed out in ref. [44], their relation goes to the heart of one of the difficulties in traditional approaches to classical field theory with point sources. Two particles that scatter in e.g. classical electrodynamics exchange momentum via their interaction with the electromagnetic field. In the classical context, this is described by the Lorentz force. However, the energy or the momentum lost by the point particles to radiation is not accounted for by the Lorentz force. In the classical setup, momentum conservation is restored by including the additional Abraham-Lorentz-Dirac (ALD) force [143–145, 155]

and e.g. refs. [156–158] for some recent treatments. In the classical context, the inclusion of the ALD force term is associated with its own problems. In particular, it leads to issues of runaway solutions and causality violations in the description of point charges in classical EM. In contrast, in the quantum-mechanical description of charged-particle scattering these issues are absent and we will see that our results for the classical two-body dynamics in electrodynamics will conserve energy and momentum automatically. For more discussions on this point, see sections 3.5 and 5.4 of ref. [44] for a KMOC integrand level discussion of this point. The main conclusion of their analysis is that the ALD radiation reaction is automatically included in the KMOC setup via the cut-contribution where an on-shell radiation photon is exchanged. This contribution first appears at two-loop order, or $\mathcal{O}(\alpha^3)$ and was compared to the classical ALD force computation in section 6.3 of ref. [44]. Our agreement below with the $\mathcal{O}(\alpha^3)$ scattering angle computed using the ALD force [99] explicitly affirms these conclusions.

3 Conservative dynamics at $\mathcal{O}(\alpha^3)$

3.1 Conservative scattering amplitudes

In this section we give the results for the tree level, one-loop and two-loop scattering amplitudes in scalar QED in the conservative sector. We combine the integrands derived in section 2.2 with the integration techniques sketched in section 2.3. A detailed account of the potential region integrals is found in refs. [39, 40, 76]. All potential region L -loop amplitudes will henceforth be denoted by $\mathcal{A}_{4,(p)}^{(L)}$.

The tree-level amplitude can be obtained from eq. (2.7) by switching from the soft variables y , and \bar{m}_1 to σ and m_i via the relations from subsection 2.1

$$\mathcal{A}_{4,(p)}^{(0)} = -(4\pi\alpha q_1 q_2) \frac{4m_1 m_2 \sigma}{-q^2}, \tag{3.1}$$

where we use the charge normalization $\alpha = e^2/4\pi$ and denote the multiple of the elementary charge e of the massive objects by q_i . The momentum transfer is q .

The conservative one-loop amplitude can be obtained from the integrand in eq. (2.17) by taking the small- q expansion of the covariant integrand. Upon reducing the q -expanded integrals to a basis of master integrals, it is given in terms of the sum of the box and crossed box integrals, as well as two triangle integrals evaluated in the potential region. (Bubble integrals are zero in the potential region.)

$$\mathcal{A}_{4,(p)}^{(1)} = -ic_{\Pi} (I_{\Pi}^{(p)} + I_X^{(p)}) - ic_{\triangleleft} I_{\triangleleft}^{(p)} - ic_{\triangleright} I_{\triangleright}^{(p)}. \tag{3.2}$$

The coefficients are

$$c_{\Pi} = (16\pi \alpha q_1 q_2 m_1 m_2 \sigma)^2, \quad c_{\triangleleft} = -\frac{1}{2}(16\pi \alpha q_1 q_2 m_1)^2, \quad c_{\triangleright} = -\frac{1}{2}(16\pi \alpha q_1 q_2 m_2)^2. \tag{3.3}$$

Inserting the explicit values of the integrals in the potential region (see e.g. ref. [76]) yields

$$\begin{aligned}
 \mathcal{A}_{4,(p)}^{(1)} = & (4\pi\alpha q_1 q_2)^2 \frac{1}{(4\pi)^2} \left(\frac{-q^2}{\bar{\mu}^2} \right)^{-\epsilon} \left\{ \frac{1}{(-q^2)} \frac{i\pi(\sigma^2 m_1 m_2)}{2\sqrt{\sigma^2 - 1}} \frac{e^{\epsilon\gamma_E} \Gamma(-\epsilon)^2 \Gamma(1 + \epsilon)}{\Gamma(-2\epsilon)} \right. \\
 & + 8 \frac{1}{\sqrt{-q^2}} \sqrt{\pi}(m_1 + m_2) \frac{e^{\epsilon\gamma_E} \Gamma\left(\frac{1}{2} - \epsilon\right)^2 \Gamma\left(\epsilon + \frac{1}{2}\right)}{2\Gamma(1 - 2\epsilon)} \\
 & - \epsilon \frac{1}{\sqrt{-q^2}} \frac{\sqrt{\pi}(m_1 + m_2)}{(\sigma^2 - 1)} \frac{e^{\epsilon\gamma_E} \Gamma\left(\frac{1}{2} - \epsilon\right)^2 \Gamma\left(\epsilon + \frac{1}{2}\right)}{\Gamma(1 - 2\epsilon)} \\
 & \left. - \epsilon \frac{i\pi(m_1^2 + m_2^2 + 2m_1 m_2 \sigma)}{8m_1 m_2 (\sigma^2 - 1)^{3/2}} \frac{e^{\epsilon\gamma_E} \Gamma(-\epsilon)^2 \Gamma(1 + \epsilon)}{\Gamma(-2\epsilon)} \right\} + \dots,
 \end{aligned} \tag{3.4}$$

where $\bar{\mu}^2 = 4\pi e^{-\gamma_E} \mu^2$, while μ and γ_E are the dimensional regularization scale, and the Euler-Mascheroni constant, respectively. The ellipsis stand for terms with polynomial (including constant) dependence on q^2 , with or without poles in ϵ . Such terms give rise to contact interactions after Fourier transform to impact-parameter space, and are irrelevant for long-range classical physics.

Finally, the two-loop amplitude in the potential region is given by

$$\begin{aligned}
 \mathcal{A}_{4,(p)}^{(2)} = & (4\pi\alpha q_1 q_2)^3 \left(\frac{i}{(4\pi)^2} \right)^2 \left(\frac{-q^2}{\bar{\mu}^2} \right)^{-2\epsilon} \left\{ -\frac{1}{(-q^2)} \frac{32\pi^2 m^2 \nu \sigma^3}{(\sigma^2 - 1)} \left[\frac{1}{\epsilon^2} - \frac{\pi^2}{6} \right] \right. \\
 & + \frac{1}{\sqrt{-q^2}} \frac{16i\pi m}{(\sigma^2 - 1)^{1/2}} \left[\frac{1}{\epsilon} - 2\log(2) - \frac{4\sigma^3}{\sigma^2 - 1} + \mathcal{O}(\epsilon) \right] \\
 & \left. + \frac{8\pi^2}{\epsilon} \left[\frac{2\nu(1 - \sigma^2 - \sigma^4) + (1 - 2\nu)(\sigma - 2\sigma^3)}{\nu(\sigma^2 - 1)^2} + \mathcal{O}(\epsilon) \right] \right\} + \dots
 \end{aligned} \tag{3.5}$$

where we have used the total mass, m , and symmetric mass ratio, ν ,

$$m = m_1 + m_2, \quad \nu = \frac{m_1 m_2}{(m_1 + m_2)^2}. \tag{3.6}$$

3.2 Eikonal approach to classical conservative scattering

Armed with the conservative amplitude through two loops, we may compute the eikonal phase. Traditionally, one Fourier transforms the amplitudes to impact-parameter space in order to extract the eikonal phase. Here, following ref. [76], we instead use the eikonal exponentiation directly in momentum space. This comes at the cost of products in impact-parameter space becoming convolutions in momentum space. However, all needed convolutions have already been evaluated in ref. [76]. We summarize the result of our calculation of the eikonal phase (Our convention for eikonal phase differs by a factor of 2 from that

of [76] and is consistent with the definition of the eikonal in the soft region of section 4.2.)

$$2\delta_{(p)}^{(0)}(\sigma, \mathbf{q}_\perp) = -(4\pi\alpha q_1 q_2) 4m_1 m_2 \sigma \frac{1}{\mathbf{q}_\perp^2}, \quad (3.7)$$

$$2\delta_{(p)}^{(1)}(\sigma, \mathbf{q}_\perp) = (4\pi\alpha q_1 q_2)^2 \frac{(m_1 + m_2)}{4} \frac{1}{|\mathbf{q}_\perp|}, \quad (3.8)$$

$$2\delta_{(p)}^{(2)}(\sigma, \mathbf{q}_\perp) = (4\pi\alpha q_1 q_2)^3 \frac{2\nu + (1 - 2\nu)\sigma}{16(\sigma^2 - 1)\nu} \log(\mathbf{q}_\perp^2), \quad (3.9)$$

where we use the $D - 2$ -dimensional spacelike vector, \mathbf{q}_\perp , transverse to the scattering plane, satisfying $\mathbf{q}_\perp^2 = -q^2$. Finally, we can perform the Fourier transform to obtain the more familiar eikonal phase in impact-parameter space

$$\delta(\sigma, \mathbf{b}_e) = \frac{1}{4m_1 m_2 \sqrt{\sigma^2 - 1}} \int \frac{d^{D-2} \mathbf{q}_\perp}{(2\pi)^{D-2}} e^{i\mathbf{b}_e \cdot \mathbf{q}_\perp} \delta(\sigma, \mathbf{q}_\perp), \quad (3.10)$$

with the result

$$2\delta_{(p)}^{(0)}(\sigma, \mathbf{b}_e) = (4\pi\alpha q_1 q_2) \frac{\sigma}{4\pi\sqrt{\sigma^2 - 1}} \log(\mathbf{b}_e^2), \quad (3.11)$$

$$2\delta_{(p)}^{(1)}(\sigma, \mathbf{b}_e) = (4\pi\alpha q_1 q_2)^2 \frac{1}{32\pi m\nu\sqrt{\sigma^2 - 1}} \frac{1}{|\mathbf{b}_e|}, \quad (3.12)$$

$$2\delta_{(p)}^{(2)}(\sigma, \mathbf{b}_e) = -(4\pi\alpha q_1 q_2)^3 \frac{(2\nu + (1 - 2\nu)\sigma)}{64\pi^3 m^2 \nu^2 \sqrt{\sigma^2 - 1}} \frac{1}{\mathbf{b}_e^2}, \quad (3.13)$$

where we have dropped terms that do not contribute to the classical scattering angle. As discussed below (see eq. (3.23)), the eikonal impact parameter \mathbf{b}_e is distinct from the geometric impact parameter \mathbf{b} .

3.3 Conservative eikonal phase, scattering angle, and two-body Hamiltonian

The stationary phase approximation of the Fourier transform of the exponentiated impact-parameter amplitude back to momentum space

$$\mathcal{A}(\sigma, -q^2) = \int d^{D-2} \mathbf{b}_e \left(e^{2i\delta(\sigma, \mathbf{b}_e)} - 1 \right) e^{-i\mathbf{q} \cdot \mathbf{b}_e} \quad (3.14)$$

yields the relation

$$\mathbf{q} = -\frac{\partial}{\partial \mathbf{b}_e} 2\delta(\sigma, \mathbf{b}_e). \quad (3.15)$$

The magnitude of \mathbf{q} is related to the scattering angle χ and the magnitude of the three-momentum \mathbf{p} in the center-of-mass frame by

$$|\mathbf{q}| = 2|\mathbf{p}| \sin \frac{\chi}{2}. \quad (3.16)$$

From this, we may now calculate the gravitational scattering angle from the eikonal phase using the formula

$$\sin \frac{\chi}{2} = -\frac{1}{2|\mathbf{p}|} \frac{\partial}{\partial |\mathbf{b}_e|} 2\delta(\sigma, \mathbf{b}_e). \quad (3.17)$$

where in terms of the center of mass energy $E = \sqrt{s}$ and/or σ

$$p_\infty \equiv |\mathbf{p}| = \frac{m_1 m_2 \sqrt{\sigma^2 - 1}}{E} = \frac{m_1 m_2 \sqrt{\sigma^2 - 1}}{\sqrt{m_1^2 + m_2^2 + 2m_1 m_2 \sigma}} = \frac{m\nu \sqrt{\sigma^2 - 1}}{\sqrt{1 + 2\nu(\sigma - 1)}}. \quad (3.18)$$

Using this formula we find the following result for the scattering angle

$$\chi_{(p)}^{(0)} = -\frac{\alpha q_1 q_2}{|\mathbf{b}_e|} \frac{2\sigma}{|\mathbf{p}| \sqrt{\sigma^2 - 1}}, \quad (3.19)$$

$$\chi_{(p)}^{(1)} = \frac{(\alpha q_1 q_2)^2}{|\mathbf{b}_e|^2} \frac{\pi}{2|\mathbf{p}| m\nu \sqrt{\sigma^2 - 1}}, \quad (3.20)$$

$$\chi_{(p)}^{(2)} = -\frac{(\alpha q_1 q_2)^3}{|\mathbf{b}_e|^3} \left[\frac{\sigma^3}{3|\mathbf{p}|^3 (\sigma^2 - 1)^{3/2}} + \frac{2(2\nu + (1 - 2\nu)\sigma)}{|\mathbf{p}| m^2 \nu^2 \sqrt{\sigma^2 - 1}} \right]. \quad (3.21)$$

Comparing the result in eqs. (3.19)–(3.20), we find agreement (up to conventions) with Westpfahl [33]. It is useful to write the formulae in terms of the angular momentum, J , as defined via

$$J = |\mathbf{b} \times \mathbf{p}| = |\mathbf{b}| |\mathbf{p}|, \quad (3.22)$$

where \mathbf{b} is the asymptotic impact parameter perpendicular to the incoming center of mass momentum \mathbf{p} . As noted earlier, this is not the impact parameter, \mathbf{b}_e , relevant to the eikonal phase and pointing in the direction of the momentum transfer \mathbf{q} . The magnitude of \mathbf{b} and \mathbf{b}_e are then related by

$$|\mathbf{b}| = |\mathbf{b}_e| \cos \frac{\chi}{2}, \quad (3.23)$$

so that the angular momentum is

$$J = |\mathbf{b}_e| |\mathbf{p}| \cos \frac{\chi}{2}. \quad (3.24)$$

This difference is unimportant at leading orders, and it will only matter at order J^{-3} . Using the relation (3.24) we find the scattering angle in terms of the angular momentum

$$\begin{aligned} \chi_{(p)}^{(0)} &= -\frac{\alpha q_1 q_2}{J} \frac{2\sigma}{\sqrt{\sigma^2 - 1}}, \\ \chi_{(p)}^{(1)} &= \frac{(\alpha q_1 q_2)^2}{J^2} \frac{\pi}{2\sqrt{1 + 2\nu(\sigma - 1)}}, \\ \chi_{(p)}^{(2)} &= \frac{(\alpha q_1 q_2)^3}{J^3} \frac{4\nu(3 - 3\sigma^2 + \sigma^4) + (1 - 2\nu)(6\sigma - 4\sigma^3)}{3(1 + 2\nu(\sigma - 1))(\sigma^2 - 1)^{3/2}}. \end{aligned} \quad (3.25)$$

One can write the conservative Hamiltonian for a system of two spinless charges in an expansion in powers of the electromagnetic coupling as

$$\begin{aligned} H(\mathbf{r}^2, \mathbf{p}^2) &= \sqrt{\mathbf{p}^2 + m_1^2} + \sqrt{\mathbf{p}^2 + m_2^2} \\ &+ c_1(\mathbf{p}^2) \frac{\tilde{\alpha}}{|\mathbf{r}|} + c_2(\mathbf{p}^2) \left(\frac{\tilde{\alpha}}{|\mathbf{r}|} \right)^2 + c_3(\mathbf{p}^2) \left(\frac{\tilde{\alpha}}{|\mathbf{r}|} \right)^3 + \dots, \end{aligned} \quad (3.26)$$

where $\tilde{\alpha}=4\pi\alpha q_1 q_2$ and the $c_i(\mathbf{p}^2)$ are yet to be determined coefficients. Such a Hamiltonian was used in ref. [40], to obtain a related expansion of the classical scattering angle

$$\chi = \frac{P_1}{p_\infty} \left(\frac{\tilde{\alpha}}{J} \right) + \frac{\pi}{2} P_2 \left(\frac{\tilde{\alpha}}{J} \right)^2 - \frac{P_1^3 - 12p_\infty^2 P_1 P_2 - 24p_\infty^4 P_3}{12p_\infty^3} \left(\frac{\tilde{\alpha}}{J} \right)^3 + \mathcal{O} \left((\tilde{\alpha}/J)^4 \right), \quad (3.27)$$

where p_∞ was defined in eq. (3.18). The P_i coefficients in the scattering angle are the natural expansion coefficients for the radial momentum $p_r^2(r)$ (see section 11 of [40] for details in the context of GR), but are also related to the c_i coefficients in the Hamiltonian via [40]

$$P_1 = -2E\xi\bar{c}_1, \quad (3.28)$$

$$P_2 = -2E\xi\bar{c}_2 + (1 - 3\xi)\bar{c}_1^2 + 4E^2\xi^2\bar{c}_1\bar{c}'_1, \quad (3.29)$$

$$P_3 = -2E\xi\bar{c}_3 + 2(1 - 3\xi)\bar{c}_1\bar{c}_2 - 4E^3\xi^3\bar{c}_1 \left(2\bar{c}'_1{}^2 + \bar{c}_1\bar{c}''_1 \right) + 4E^2\xi^2 \left(\bar{c}_2\bar{c}'_1 + \bar{c}_1\bar{c}'_2 \right) - 6E(1 - 3\xi)\xi\bar{c}_1^2\bar{c}'_1 + \frac{(1 - 4\xi)\bar{c}_1^3}{E}, \quad (3.30)$$

where $\bar{c}_i \equiv c_i(p_\infty^2)$, primes denote derivatives with respect to the argument, $E = E_1 + E_2 = m\sqrt{1 + 2\nu(\sigma - 1)}$ and $\xi = E_1 E_2 / E^2 = \frac{\nu(\nu(\sigma - 1)^2 + \sigma)}{(1 + 2\nu(\sigma - 1))^2}$. Conversely, one may start from our scattering angles in eq. (3.25), deduce the P_i coefficients in eq. (3.27) up to $\mathcal{O}(\alpha^3)$

$$P_1 = -\frac{2m\nu\sigma}{(4\pi)\Gamma}, \quad P_2 = \frac{1}{(4\pi)^2} \frac{1}{\Gamma}, \quad P_3 = \frac{(\Gamma - 1)\sigma + 2\nu(\sigma - 1)}{(4\pi)^3 \Gamma m\nu(\sigma^2 - 1)}, \quad (3.31)$$

where we have defined $\Gamma = E/m = \sqrt{1 + 2\nu(\sigma - 1)}$. Relatedly, the coefficients in the expansion of the scattering angle can also be expressed via suitably defined finite parts of scattering amplitudes (see discussion around eq. (12) of [39]) in terms of slightly rescaled coefficients \tilde{d}_i which differ from P_i by powers of p_∞ , $\tilde{d}_i = p_\infty^{i-2} P_i$.⁶

$$\chi = \tilde{d}_1 \left(\frac{\tilde{\alpha}}{J} \right) + \frac{\pi}{2} \tilde{d}_2 \left(\frac{\tilde{\alpha}}{J} \right)^2 - \left(\frac{\tilde{d}_1^3}{12} - \tilde{d}_1 \tilde{d}_2 + 2\tilde{d}_3 \right) \left(\frac{\tilde{\alpha}}{J} \right)^3 + \mathcal{O} \left((\tilde{\alpha}/J)^4 \right), \quad (3.32)$$

where the coefficients now read

$$\tilde{d}_1 = -\frac{2\sigma}{(4\pi)\sqrt{\sigma^2 - 1}}, \quad \tilde{d}_2 = \frac{1}{(4\pi)^2 \Gamma}, \quad \tilde{d}_3 = \frac{(\Gamma - 1)(1 + \Gamma + \sigma)}{(4\pi)^3 \Gamma^2 \sqrt{\sigma^2 - 1}}. \quad (3.33)$$

An interesting feature is that two-loop function \tilde{d}_3 vanishes in the test mass limit $\nu \rightarrow 0$ ($\Gamma \rightarrow 1$), i.e. $\tilde{d}_3 \xrightarrow{\nu \rightarrow 0} 0$. This is due to the fact that $\Gamma - 1$ starts at $\mathcal{O}(\nu)$ in the test mass expansion. Crucially, $\tilde{d}_3 = 0$ implies that the $\mathcal{O}(\alpha^3)$ test-body Hamiltonian is fully determined by lower-loop information. In fact, in the test-body limit, the scattering angle is

⁶We use \tilde{d}_i rather than d_i to signal slight normalization differences by factors of π and the coupling constant compared to [39].

computable exactly to all orders in the coupling (see e.g. ref. [103]⁷ and references therein)

$$\begin{aligned} \chi_{\text{test}} &= \frac{J}{\sqrt{J^2 - (\alpha q_1 q_2)^2}} \left(\pi + 2 \arctan \left[\frac{-(\alpha q_1 q_2)}{\beta \sqrt{J^2 - (\alpha q_1 q_2)^2}} \right] \right) - \pi, \\ &= -\frac{2\alpha q_1 q_2}{\beta J} + \frac{\pi \alpha^2 q_1^2 q_2^2}{2J^2} - \frac{2\alpha^3 (3\beta^2 - 1) q_1^3 q_2^3}{3\beta^3 J^3} + \frac{3\pi \alpha^4 q_1^4 q_2^4}{8J^4} + \mathcal{O}(\alpha^5), \end{aligned} \quad (3.34)$$

where $\beta = \sqrt{\sigma^2 - 1}/\sigma$ is the velocity. With the test-body angle available to all orders in the coupling constant, we can investigate the angle relation of eq. (3.27) for the P_i to higher orders in perturbation theory. At $\mathcal{O}(\alpha^4)$, we would find (see eq. (11.25) of [40])

$$\begin{aligned} \chi &= (3.27) + \frac{3\pi}{8} \left(P_2^2 + 2P_1 P_3 + 2p_\infty^2 P_4 \right) \left(\frac{\tilde{\alpha}}{J} \right)^4 + \mathcal{O}((\tilde{\alpha}/J)^5), \\ &= (3.32) + \frac{3\pi}{8} \left(\tilde{d}_2^2 + 2\tilde{d}_1 \tilde{d}_3 + 2\tilde{d}_4 \right) \left(\frac{\tilde{\alpha}}{J} \right)^4 + \mathcal{O}((\tilde{\alpha}/J)^5) \end{aligned} \quad (3.35)$$

Comparing the explicit angle in the test-body limit (3.34) to the expansion in eq. (3.35), we see that $\tilde{d}_3 = \tilde{d}_4 = 0$. Indeed, all $\tilde{d}_{i>2} = 0$ vanish in the test-body limit which in turn implies that the higher Hamiltonian coefficients $c_{i>2}$ are equally determined by at most one-loop data. In light of this discussion, the reason there is a simple closed form solution for the scattering angle is connected to the simplicity of the test mass Hamiltonian.

For the sake of completeness, we also tabulate the c_i coefficients in the Hamiltonian or general mass dependence up to $\mathcal{O}(\alpha^3)$. This yields

$$c_1 = \frac{1}{4\pi(2\Gamma^2\xi^2)} (2\Gamma^2\xi^2\tilde{\nu}), \quad (3.36)$$

$$c_2 = \frac{1}{(4\pi)^2 m(2\Gamma^2\xi^2)} \left(-\xi + 2\Gamma\xi\tilde{\nu} - \Gamma\xi(1-\xi)\tilde{\nu}^2 \right), \quad (3.37)$$

$$\begin{aligned} c_3 &= \frac{1}{(4\pi)^3 m^2(2\Gamma^2\xi^2)} \left\{ \frac{\sigma^2}{1-\sigma^2} \left(\frac{\Gamma-1}{\Gamma} \right) \frac{1}{\tilde{\nu}} - \frac{1+\sigma+2\Gamma\xi}{(1+\sigma)\Gamma} \right. \\ &\quad \left. + \frac{2\Gamma+1-\xi}{\Gamma} \tilde{\nu} - (3-4\xi)\tilde{\nu}^2 + (1-2\xi)\tilde{\nu}^3 \right\}, \end{aligned} \quad (3.38)$$

where $\tilde{\nu} = \frac{\sigma\nu}{\Gamma^2\xi} = \frac{\sigma(1+2\nu(\sigma-1))}{\nu(\sigma-1)^2+\sigma}$.

3.4 Conservative impulse and scattering angle via KMOC

Besides extracting the classical observables via the eikonal approach discussed in section 3.2 or in terms of a classical Hamiltonian (see section 3.3), we have also computed the conservative electromagnetic impulse within the KMOC framework, generally discussed in section 2.5. In the conservative setting, energy is conserved in the scattering process, so that there is no radiated momentum or energy loss to consider. In terms of the method of regions, this is encoded in the fact that all photons are purely potential and can never

⁷In comparison to ref. [103], our scattering angle is defined to go to zero in the absence of interactions ($\alpha \rightarrow 0$) which explains the additional $-\pi$. Our conventions for the charges lead to an additional sign in the argument of the arctan.

go on-shell, so that the radiation cuts in eq. (2.47) are always absent. Likewise, for the impulse, we only have to consider elastic processes without exchanged messenger particles in the *real* contribution in eq. (2.40).

Due to energy conservation in the conservative sector, it suffices to determine the transverse impulse only and the longitudinal part is completely determined by the on-shell conditions and momentum conservation of the process

$$(p_i + \Delta p_i)^2 = p_i^2 \quad \Delta p_1 + \Delta p_2 = 0. \quad (3.39)$$

Employing generalized unitarity, we constructed the relevant conservative integrand to extract the transverse impulse kernel from eq. (2.45) where only the first two diagrams of figure (2) are relevant at $\mathcal{O}(\alpha^3)$. Using the same integration and assembly pipeline that has already produced the conservative gravitational results in ref. [47] together with the potential region values of the master integrals from ref. [76], we obtain the transverse impulse on particle 1 at two loops⁸

$$\Delta p_{1,\perp}^{\mu,\text{cons.}} = (\alpha q_1 q_2)^3 \frac{2(2m_1 m_2 (\sigma^4 - \sigma^2 + 1) + (m_1^2 + m_2^2)\sigma) b^\mu}{m_1^2 m_2^2 (\sigma^2 - 1)^{5/2}} \frac{1}{|b|^4}. \quad (3.40)$$

The conservative longitudinal impulse at $\mathcal{O}(\alpha^3)$ is

$$\Delta p_{1,u}^{\mu,\text{cons.}} = (\alpha q_1 q_2)^3 \frac{\pi (m_1 + m_2) \sigma}{m_1 m_2 |b|^3 (\sigma^2 - 1)} \left(\frac{\check{u}_2^\mu}{m_2} - \frac{\check{u}_1^\mu}{m_1} \right). \quad (3.41)$$

Both the longitudinal and transverse impulse agree with the ones obtained from the scattering angles (3.25) and the help of the parametrization of the impulse in terms of the conservative scattering angle of appendix B in ref. [47]. We also agree with the recent computation of the impulse obtained by solving classical equations of motion [99].

In comparing to the gravitational result [47], in electrodynamics there is no $\text{arcsinh}\sqrt{\frac{\sigma-1}{2}}$ high-energy singularity in the transverse impulse, which also renders this feature absent from the scattering angle. At high energies, i.e. large $\sigma \gg 1$, and fixed impact parameter b , the leading large sigma behavior of the transverse and longitudinal impulse scale like $1/\sigma$ and $1/\sigma^2$, respectively. For the longitudinal impulse, one has to take the definition of the \check{u}_i $\sigma \gg 1$ $1/\sigma$ in eq. (2.43) into account.

4 Radiative dynamics at $\mathcal{O}(\alpha^3)$

4.1 Radiative scattering amplitudes

In this section we give the results for the scattering amplitudes in the soft region that includes radiation effects by combining the integrands from section 2.2 with the integration techniques sketched in section 2.3. Detailed results of all soft-region integrals can be found

⁸We drop the explicit label of the perturbative order of the observable (see eq. (2.36)) for brevity. The same information is encoded in the order of α .

in ref. [47]. The tree-level amplitude remains

$$\mathcal{A}_4^{(0)}(p_1, p_2, p_3, p_4) = \begin{array}{c} p_2 \text{ --- } p_3 \\ | \\ p_1 \text{ --- } p_4 \end{array} = -(4\pi\alpha q_1 q_2) \frac{4m_1 m_2 \sigma}{-q^2}, \quad (4.1)$$

The one-loop amplitude in the soft region is

$$\begin{aligned} \mathcal{A}_4^{(1)}(p_1, p_2, p_3, p_4) &= (4\pi\alpha q_1 q_2)^2 \left[i \left(\frac{1}{4\pi} \right)^{2-\epsilon} \frac{e^{-\gamma\epsilon}}{(-q^2)^\epsilon} \right] \left[\frac{4\pi^2 m_1 m_2 (z^2 + 1)^2 e^{\gamma\epsilon} \csc(\pi\epsilon) \Gamma(-\epsilon)}{(-q^2) z (z^2 - 1) \Gamma(-2\epsilon)} \right. \\ &+ \frac{i\pi^2 (m_1 + m_2) 4^{\epsilon+1} e^{\gamma\epsilon} \left(4(z^2 + 1)^2 \epsilon - (z^2 - 1)^2 \right) \sec(\pi\epsilon)}{\sqrt{-q^2} (z^2 - 1)^2 \Gamma(1 - \epsilon)} \\ &\left. + \frac{\pi^{3/2} 2^{2\epsilon+1} e^{\gamma\epsilon} \csc(\pi\epsilon)}{\Gamma\left(\frac{3}{2} - \epsilon\right) m_1 m_2 (z^2 - 1)^3} f(z, \epsilon) + \mathcal{O}(|q|) \right], \end{aligned} \quad (4.2)$$

where γ is the Euler-Mascheroni constant and

$$\begin{aligned} f(z, \epsilon) &= \left[2\pi \left(m_1^2 + m_2^2 \right) z \left(z^2 + 1 \right)^2 \epsilon (2\epsilon - 1) + m_1 m_2 \left\{ 4 \left(z^2 + 1 \right)^2 \left((\pi + 2i) z^2 - 2i + \pi \right) \epsilon^2 \right. \right. \\ &- 2 \left(\pi \left(z^2 + 1 \right)^3 + 2i \left(z^2 - 1 \right)^3 \right) \epsilon \\ &+ 2i \left(z^2 + 1 \right) (2\epsilon - 1) \left(2 \left(z^2 + 1 \right)^2 \epsilon - z^4 + 6z^2 - 1 \right) \log(z) \\ &\left. \left. - i \left(z^6 + 5z^4 - 5z^2 - 1 \right) \right\} \right], \end{aligned} \quad (4.3)$$

is written in terms of z , related to $\sigma = \frac{1+z^2}{2z}$ in order to rationalize square roots such as $\sqrt{\sigma^2 - 1} = \frac{1-z^2}{2z}$. When converting the computations in terms of the soft-variables y, x, \bar{m}_i to the original masses m_i and σ, z , one has to be careful to take into account subleading $\mathcal{O}(q^2)$ terms in the conversion in order to obtain the correct expression for the one-loop quantum piece.

The relevant parts of the two-loop amplitude are

$$\frac{\mathcal{A}_4^{(2)}(p_1, p_2, p_3, p_4)}{(4\pi\alpha)^3} = \left[i \left(\frac{1}{4\pi} \right)^{2-\epsilon} \frac{e^{-\gamma\epsilon}}{(-q^2)^\epsilon} \right]^2 \left[\frac{a_{-1,-2}^{(2)}}{(-q^2) \epsilon^2} + \frac{a_{-1,-1}^{(2)}}{(-q^2) \epsilon} + \frac{a_{-\frac{1}{2},-1}^{(2)}}{\sqrt{-q^2} \epsilon} + \frac{a_{0,-2}^{(2)}}{\epsilon^2} + \frac{a_{0,-1}^{(2)}}{\epsilon} \right], \quad (4.4)$$

where the two-loop amplitude coefficients $a_{i,j}^{(2)}$ are labeled by the order in the q and ϵ expansion. In principle, we also have access to higher-order terms in the ϵ and q expansion, but they do not play a role for the purpose of our discussion here. The expression for the classical term $a_{0,-1}^{(2)}$ is rather lengthy, so we do not display it here. (We supply all expressions in computer readable form as an ancillary file.) The classical term $a_{0,-1}^{(2)}$ contains contributions from both the charge sector proportional to $q_1^3 q_2^3$ as well as from the

mushroom topologies $q_i^4 q_j^2$. In contrast, the classically divergent terms as well as the $1/\epsilon^2$ coefficient of the classical piece are entirely within the $q_1^3 q_2^3$ sub-sector,

$$a_{-1,-2}^{(2)} = -(q_1 q_2)^3 \frac{16\pi^2 m_1 m_2 (z^2 + 1)^3}{z (z^2 - 1)^2}, \quad a_{-1,-1}^{(2)} = 0, \quad (4.5)$$

$$a_{-\frac{1}{2},-1}^{(2)} = (q_1 q_2)^3 \frac{16i\pi^3 (m_1 + m_2) (z^2 + 1)}{(z^2 - 1)}, \quad (4.6)$$

$$a_{0,-2}^{(2)} = (q_1 q_2)^3 \frac{8i\pi (z^2 + 1) (3z^6 + 7z^4 - 7z^2 - 3 + 2(z^6 - 9z^4 - 9z^2 + 1) \log(z))}{(z^2 - 1)^4}. \quad (4.7)$$

Again, all results are written in the terms of the z variable that rationalizes $\sqrt{\sigma^2 - 1}$.

4.2 Eikonal approach to classical scattering including radiation effects

In a first implementation of radiative effects in scalar QED at $\mathcal{O}(\alpha^3)$, we follow the eikonal approach that has been successfully used in ref. [148] to extract the classical scattering angle in gravity. The steps in their derivation are independent of the theory under consideration as long as they admit a suitable classical limit. It is therefore natural to expect that we can follow section 2.2 of ref. [148] for scalar QED. As we will show, this expectation is indeed correct. Since the physical intuition behind the eikonal approach has already been discussed extensively by Di Vecchia et al. [148], we restrict ourselves to only the most important formulae. At the heart of the eikonal approach is the expected exponentiation of certain parts of the scattering amplitude in impact-parameter space

$$1 + i\tilde{\mathcal{A}}(s, b_e) = (1 + 2i\Delta(s, b_e))e^{2i\delta(s, b_e)}, \quad (4.8)$$

where $\delta(s, b_e)$ is the classical eikonal phase and $\Delta(s, b_e)$ is a quantum remainder that starts with one-loop contributions. (We follow the notation of ref. [148] but keep in mind that we express s in terms of σ or z .) Let us note, that it is a priori unclear what part of the amplitude exponentiates beyond leading order. In the conservative sector discussed in section 3.2, there is an good argument based on elastic unitarity, that the amplitude (including quantum terms) exponentiates. Here, we follow the prescription of ref. [148] that exponentiate strictly classical terms and all quantum corrections are assigned to $\Delta(s, b_e)$. However, from the conservative perspective, one could expect that certain quantum terms that originate from the potential region should still exponentiate and lead to quantum corrections of the classical eikonal phase $\delta(s, b_e)$ and only quantum radiation pieces need not resum to a phase. We do not pursue this separation further and leave a detailed investigation to future work. The momentum-space amplitude $\mathcal{A}(s, -q^2)$ is Fourier-transformed to the $D - 2$ -dimensional impact-parameter space, conjugate to the (space-like) momentum-transfer q

$$\tilde{\mathcal{A}}(s, b_e) = \int \frac{d^{D-2}q}{(2\pi)^{D-2}} \frac{\mathcal{A}(s, -q^2)}{4m_1 m_2 \sqrt{\sigma^2 - 1}} e^{ib_e \cdot q}. \quad (4.9)$$

Here, we distinguish the eikonal impact parameter b_e from the asymptotic impact parameter b related by the geometric identity

$$b_e = \frac{b}{\cos \frac{\chi}{2}}, \tag{4.10}$$

where χ is the scattering angle. The momentum-space scattering amplitude $\mathcal{A}(s, -q^2)$ entering in eq. (4.9) has an expansion in terms of the coupling constant (loop-expansion) as well as an expansion in powers of $-q^2$. Via standard Fourier integrals, the power-series expansion in $-q^2$ gets converted to a similar expansion in impact-parameter space

$$\mathcal{A}_4^{(0)} = \frac{a_{-1}^{(0)}}{-q^2} \quad \rightarrow \quad \tilde{\mathcal{A}}_4^{(0)} = \frac{\tilde{a}_{-1}^{(0)}}{(-b_e^2)^{-\epsilon}}, \tag{4.11}$$

$$\mathcal{A}_4^{(1)} = \frac{a_{-1}^{(1)}}{(-q^2)^{1+\epsilon}} + \frac{a_{-1/2}^{(1)}}{(-q^2)^{\frac{1}{2}+\epsilon}} + \frac{a_0^{(1)}}{(-q^2)^\epsilon} \quad \rightarrow \quad \tilde{\mathcal{A}}_4^{(1)} = \frac{\tilde{a}_{-1}^{(1)}}{(-b_e^2)^{-2\epsilon}} + \frac{\tilde{a}_{-1/2}^{(1)}}{(-b_e^2)^{\frac{1}{2}-2\epsilon}} + \frac{\tilde{a}_0^{(1)}}{(-b_e^2)^{1-2\epsilon}}, \tag{4.12}$$

$$\mathcal{A}_4^{(2)} = \frac{a_{-1}^{(2)}}{(-q^2)^{1+2\epsilon}} + \frac{a_{-1/2}^{(2)}}{(-q^2)^{\frac{1}{2}+2\epsilon}} + \frac{a_0^{(2)}}{(-q^2)^{2\epsilon}} \quad \rightarrow \quad \tilde{\mathcal{A}}_4^{(2)} = \frac{\tilde{a}_{-1}^{(2)}}{(-b_e^2)^{-3\epsilon}} + \frac{\tilde{a}_{-1/2}^{(2)}}{(-b_e^2)^{\frac{1}{2}-3\epsilon}} + \frac{\tilde{a}_0^{(2)}}{(-b_e^2)^{1-3\epsilon}}, \tag{4.13}$$

where the impact-parameter space coefficients $\tilde{a}_j^{(\ell)}$ are directly related to the momentum-space expressions around $D = 4 - 2\epsilon$ dimensions via

$$\int \frac{d^{D-2}q}{(2\pi)^{D-2}} \frac{e^{ib_e \cdot q}}{(-q^2)^\alpha} = \frac{\Gamma(D/2 - 1 - \alpha)}{2^{2\alpha+2}(\pi)^{\frac{D-2}{2}} \Gamma(\alpha)} \frac{1}{(-b_e^2)^{\frac{D-2-2\alpha}{2}}}. \tag{4.14}$$

Furthermore, the $a_i^{(\ell)}$ are simply related to the $a_{i,j}^{(\ell)}$ of eqs. (4.1), (4.2), and (4.4). Expanding the right-hand-side of the eikonal ansatz in eq. (4.8) perturbatively in the coupling α

$$\delta = \delta^{(0)} + \delta^{(1)} + \delta^{(2)} + \dots, \quad \Delta = \Delta^{(1)} + \dots, \tag{4.15}$$

one can match both sides of eq. (4.8) to the desired order in α to determine the eikonal quantities in terms of fixed-order amplitude results. Note that all classically divergent (or ‘super-classical’) terms are completely determined by lower order data and serve as non-trivial cross-check of the computation. Equipped with the eikonal phase, one can Fourier-transform back to momentum space which allows for the identification of the *classical* momentum transfer Q^μ from a stationary-phase approximation

$$Q^\mu = -\frac{\partial \text{Re } 2\delta(s, b_e)}{\partial b_e^\mu}, \tag{4.16}$$

which is related to the scattering angle χ via

$$|Q| = 2p \sin \frac{\chi}{2}, \tag{4.17}$$

where $p = \frac{\sqrt{\sigma^2 - 1} m_1 m_2}{\sqrt{m_1^2 + m_2^2 + 2m_1 m_2 \sigma}}$ is the asymptotic center of mass momentum.

In terms of the asymptotic impact parameter that is tied to the center-of-mass angular momentum $J = p b$ (see eq. (4.10)), the scattering angle is

$$\tan \frac{\chi}{2} = -\frac{1}{2p} \frac{\partial 2 \operatorname{Re} \delta}{\partial b}. \quad (4.18)$$

We can now take the perturbative expansion of eq. (4.8) together with the explicit values of the tree-, one-loop, and two-loop amplitudes in momentum space of eqs. (4.1), (4.2), and (4.4) to convert the variables to the normal masses m_i and to σ in order to obtain the explicit values for the $a_i^{(\ell)}(s)$ coefficients in eq. (4.11) from which we can extract the eikonal parameters

$$\delta^{(0)}(s, b_e) = \frac{1}{(-b_e^2)^{-\epsilon}} \frac{\pi^\epsilon \Gamma(-\epsilon)}{32\pi m_1 m_2 \sqrt{\sigma^2 - 1}} a_{-1}^{(0)}, \quad (4.19)$$

$$\delta^{(1)}(s, b_e) = \frac{1}{(-b_e^2)^{\frac{1}{2}-2\epsilon}} \frac{2^{-2\epsilon} \pi^\epsilon \Gamma\left(\frac{1}{2} - 2\epsilon\right)}{16\pi m_1 m_2 \sqrt{\sigma^2 - 1} \Gamma\left(\epsilon + \frac{1}{2}\right)} a_{-1/2}^{(1)}, \quad (4.20)$$

$$\delta^{(2)}(s, b_e) = \frac{1}{(-b_e^2)^{1-3\epsilon}} \frac{1}{2m_1 m_2} \left[\frac{4^{-2\epsilon} \pi^\epsilon \Gamma(1 - 3\epsilon)}{4\pi \sqrt{\sigma^2 - 1} \Gamma(2\epsilon)} a_0^{(2)} - i \frac{2^{-2\epsilon} \pi^{2\epsilon} \Gamma(1 - 2\epsilon) \Gamma(-\epsilon)}{64\pi^2 m_1 m_2 (\sigma^2 - 1) \Gamma(\epsilon)} a_{-1}^{(0)} a_0^{(1)} \right], \quad (4.21)$$

and the one-loop quantum remainder,

$$\Delta^{(1)}(s, b_e) = \frac{1}{(-b_e^2)^{1-2\epsilon}} \frac{2^{-2\epsilon} \pi^\epsilon \Gamma(1 - 2\epsilon)}{8\pi m_1 m_2 \sqrt{\sigma^2 - 1} \Gamma(\epsilon)} a_0^{(1)}. \quad (4.22)$$

We note that the imaginary part of the two-loop eikonal, $\delta^{(2)}$, still contains a $1/\epsilon$ infrared singularity (due to the $1/\epsilon^2$ contribution of $a_0^{(2)}$ in eq. (4.22)), consistent with a similar feature in gravity [148], whereas the real part of the phase which is relevant for the physical scattering angle is IR finite.

With the explicit values of the eikonal parameters at hand, we can take eq. (4.18), convert the eikonal impact parameter in eq. (4.19) with the help of eq. (4.10), and perturbatively expand the angle $\chi = \chi^{(0)} + \chi^{(1)} + \chi^{(2)} + \dots$. This allows us to solve eq. (4.18) order by order in the coupling in terms of expressions that we know from the scattering amplitudes. In particular, we find

$$\chi^{(0)} = -(\alpha q_1 q_2) \frac{2\sigma}{J \sqrt{\sigma^2 - 1}}, \quad (4.23)$$

$$\chi^{(1)} = (\alpha q_1 q_2)^2 \frac{\pi(m_1 + m_2)}{2J^2 \sqrt{m_1^2 + m_2^2 + 2m_1 m_2 \sigma}}, \quad (4.24)$$

$$\begin{aligned} \chi^{(2)} = & (\alpha q_1 q_2)^3 \frac{(m_1^2 + m_2^2)(6\sigma - 4\sigma^3) + 4m_1 m_2 \left(3 + (\sigma^2 - 3\sigma \sqrt{\sigma^2 - 1} - 3)\sigma^2 + 6\sigma^2 \operatorname{arcsinh} \sqrt{\frac{\sigma - 1}{2}}\right)}{3J^3 (\sigma^2 - 1)^{3/2} (m_1^2 + m_2^2 + 2m_1 m_2 \sigma)} \\ & + \alpha^3 q_1^2 q_2^2 \frac{4\sigma^2 (m_2^2 q_1^2 + m_1^2 q_2^2)}{3J^3 (m_1^2 + m_2^2 + 2m_1 m_2 \sigma)}, \end{aligned} \quad (4.25)$$

where the second line of eq. (4.25) originates from the mushroom sector. Our results are in complete agreement with those of Saketh et al. [99], once we take into account the different conventions $\chi_{\text{us}}^{(L)} = -\chi_{[99]}^{(L)}$. Before discussing these results in a bit more detail, it is beneficial to split the $\mathcal{O}(\alpha^3)$ scattering angle into conservative and radiative parts,

$$\chi^{(2)} = \chi_{\text{cons.}}^{(2)} + \chi_{\text{rad.}}^{(2)}, \quad (4.26)$$

where

$$\chi_{\text{cons.}}^{(2)} = (\alpha q_1 q_2)^3 \frac{2(\sigma(3-2\sigma^2)(m_1^2+m_2^2)+2m_1m_2(\sigma^4-3\sigma^2+3))}{3J^3(\sigma^2-1)^{3/2}(m_1^2+m_2^2+2m_1m_2\sigma)}, \quad (4.27)$$

$$\begin{aligned} \chi_{\text{rad.}}^{(2)} = & -(\alpha q_1 q_2)^3 \frac{4m_1m_2\sigma^2(\sigma\sqrt{\sigma^2-1}-2\text{arcsinh}\sqrt{\frac{\sigma-1}{2}})}{J^3(\sigma^2-1)^{3/2}(m_1^2+m_2^2+2m_1m_2\sigma)} \\ & + \alpha^3 q_1^2 q_2^2 \frac{4\sigma^2(m_2^2 q_1^2 + m_1^2 q_2^2)}{3J^3(m_1^2+m_2^2+2m_1m_2\sigma)}. \end{aligned} \quad (4.28)$$

The radiative part of the angle can also be used to extract or compare to the radiated angular momentum [141, 159] at one order lower via the linear response relation

$$\chi_{\text{rad.}} = \frac{1}{2} \frac{\partial \chi_{\text{cons.}}}{\partial J} J_{\text{rad.}} + \mathcal{O}(\alpha^4). \quad (4.29)$$

where $\chi_{\text{cons.}}$ starts at $\mathcal{O}(\alpha)$.

High-energy limit of scattering angle. Similar to the discussion in ref. [99], we can investigate the behavior of our generic scattering angles of eq. (4.25) in special kinematic limits. One interesting regime is the *high-energy limit* where the center-of-mass energy E is large, with the masses $m_1 \sim m_2$ held fixed

$$E = \sqrt{m_1^2 + m_2^2 + 2m_1m_2\sigma} \gg (m_1 + m_2), \quad m_1 \sim m_2 \text{ held fixed}. \quad (4.30)$$

This is achieved by taking $\sigma \gg 1$, where $\sigma = E^2/(2m_1m_2) + \mathcal{O}(m_i/E)$. As we will soon see explicitly, the high-energy limit (4.30) is *not* equivalent to the *massless limit* where

$$\{m_1, m_2\} \rightarrow 0, \quad \sigma = \frac{E^2 - m_1^2 - m_2^2}{2m_1m_2} \rightarrow \infty, \quad E \text{ held fixed}, \quad (4.31)$$

which is outside the range of validity of our classical approximation $m_i^2 \gg |q|^2$, since the Compton wavelength of the particles $\lambda_c \sim 1/m$ becomes large compared to the impact parameter $|b| \sim 1/|q|$, whereas classical physics requires $\lambda_c \ll |b|$. The exact details of the high-energy limit depend on the parameters that are held fixed in the scattering experiment.⁹ In particular, so far we have opted to write the scattering angle in terms of the large angular momentum J , related to the impact parameter b ,

$$J = \frac{m_1m_2\sqrt{\sigma^2-1}|b|}{\sqrt{m_1^2+m_2^2+2m_1m_2\sigma}} \xrightarrow{\text{HE}} \frac{|b|E}{2} + \mathcal{O}(1/E), \quad (4.32)$$

⁹One may consider, for example, fixing a small $\chi^{(0)} \sim \frac{q_i^2}{Eb}$ and then take the high-energy limit $E \gg m$. Instead, we choose to fix q_i and b in addition to the masses.

by an additional factor of E in the high-energy limit which shifts the overall energy dependence of the answer by overall powers of E in the conversion of L -loop results which are proportional to $1/J^{L+1}$.

We are now in the position to discuss the high-energy limit and the massless limit of the conservative and radiative scattering angles. The high-energy limit is taken according to eq. (4.30), where we express all quantities in terms of σ and expand around $\sigma \gg 1$, keeping m_1, m_2 fixed. At the end of the expansion, we identify $\sigma \simeq E^2/(2m_1m_2)$. The massless limit is taken according to eq. (4.31), by writing all quantities in terms of E (held fixed) by substituting $\sigma = (E^2 - m_1^2 - m_2^2)/(2m_1m_2)$ and series expanding for small masses $\epsilon \sim m_1 \sim m_2$. Up to $\mathcal{O}(\alpha^3)$, the leading order expressions for the high-energy limit and the massless limit coincide functionally (in each individual charge sector), but the interpretation will be *different*. We find

$$\chi_{\text{cons.}} \Big|_{\text{HE}} = \chi^{(0)} \Big|_{\text{HE}} + \chi^{(1)} \Big|_{\text{HE}} + \chi_{\text{cons.}}^{(2)} \Big|_{\text{HE}} + \mathcal{O}(\alpha^4), \quad (4.33)$$

where we have the explicit high-energy values of the scattering angles

$$\chi^{(0)} \Big|_{\text{HE}/m \rightarrow 0} = -\frac{4\alpha m_1 m_2}{E |b|} \left[\frac{q_1}{m_1} \right] \left[\frac{q_2}{m_2} \right], \quad (4.34)$$

$$\chi^{(1)} \Big|_{\text{HE}/m \rightarrow 0} = \frac{2\pi\alpha^2 m_1^2 m_2^2 (m_1 + m_2)}{E^3 |b|^2} \left[\frac{q_1}{m_1} \right]^2 \left[\frac{q_2}{m_2} \right]^2, \quad (4.35)$$

$$\chi_{\text{cons.}}^{(2)} \Big|_{\text{HE}/m \rightarrow 0} = \frac{16\alpha^3 m_1^3 m_2^3}{3E^3 |b|^3} \left[\frac{q_1}{m_1} \right]^3 \left[\frac{q_2}{m_2} \right]^3, \quad (4.36)$$

in terms of the charge-to-mass ratios $r_i \equiv q_i/m_i$. The conservative scattering angles are both well-behaved in the high-energy limit $E \rightarrow \infty$, m_i fixed, as well as in the massless limit $m_i \rightarrow 0$, E fixed. The radiative angle is more interesting,

$$\chi_{\text{rad.}}^{(2)} \Big|_{\text{HE}/m \rightarrow 0} = -\frac{16\alpha^3 m_1^3 m_2^3}{E^3 |b|^3} \left[\frac{q_1}{m_1} \right]^3 \left[\frac{q_2}{m_2} \right]^3 + \frac{8\alpha^3 m_1^2 m_2^2}{3E |b|^3} \left(\left[\frac{q_1}{m_1} \right]^4 \left[\frac{q_2}{m_2} \right]^2 + \left[\frac{q_1}{m_1} \right]^2 \left[\frac{q_2}{m_2} \right]^4 \right). \quad (4.37)$$

It is still finite in the high-energy regime, but, as has been pointed out in ref. [99], develops a mass singularity in the mushroom sector due to uncanceled $1/m_i^2$ in the second term of eq. (4.37). From our perspective, one should not take this as a true singularity of the result but rather as a breakdown of the classical massive point particle approximation which requires $|q|^2 \ll m_i^2$, or equivalently $m_i^2 |b|^2 \gg 1$, which prevents us from setting $m_i \rightarrow 0$ in our approach. Presumably, one could take into account coherence effects to discuss the classical scattering of light states [48]. There, however, the particle interpretation breaks down and one should instead talk about the scattering of classical waves described by coherent states.

Note that the mushroom contribution is dominant in the high-energy limit and behaves like $1/E$ at $\mathcal{O}(\alpha^3)$ whereas the $q_1^3 q_2^3$ sector scales like $1/E^3$ at large E . Combining the high-energy limit of the conservative angle in eq. (4.36) with the high-energy limit of the $q_1^3 q_2^3$ -sector of the radiative angle, we find

$$\chi_{q_1^3 q_2^3}^{(2)} \Big|_{\text{HE}/m \rightarrow 0} = -\frac{32\alpha^3 m_1^3 m_2^3}{3E^3 |b|^3} \left[\frac{q_1}{m_1} \right]^3 \left[\frac{q_2}{m_2} \right]^3 = \frac{\left[\chi^{(0)} \Big|_{\text{HE}/m \rightarrow 0} \right]^3}{3!}, \quad (4.38)$$

which is given in terms of the third power of the high-energy limit of the tree-level angle. The contribution from the mushroom diagrams on the other hand does not follow such an iterative structure at high energies.

As noted in the introduction, we view QED as a useful model for gravitational calculations that not only lets us test computational setups in a simpler context, but also sheds light on important physical questions. To this end, we would like to compare the results of some classical observables in electrodynamics to the ones in GR. One of the simplest places of comparison is the high-energy limit of the scattering angle. First, at tree- and one-loop level, the leading order behavior of the gravitational scattering angle is [33]

$$\chi_{\text{GR}}\Big|_{\text{HE}} = \chi_{\text{GR}}^{(0)}\Big|_{\text{HE}} + \chi_{\text{GR}}^{(1)}\Big|_{\text{HE}} + \mathcal{O}(G^3) = \frac{4GE}{|b|} + \frac{15\pi G^2 E(m_1 + m_2)}{4|b|^2} + \mathcal{O}(G^3). \quad (4.39)$$

The high-energy-limit of the tree-level gravitational scattering angle, $\chi_{\text{GR}}^{(0)}\Big|_{\text{HE}}$ is the double-copy of the QED angle with the replacement $q_i \rightarrow E$ and $\alpha \rightarrow G$. This is a direct consequence of the fact that the tree-level amplitude is dominated by the t -channel exchange diagram which is obtained as the product of two three-particle amplitudes. In the high-energy limit, these have the double-copy property. At one-loop, there is still some residual double-copy property present that is exposed by the same replacement as above. However, the numerical prefactor does not directly match anymore.

At two-loop order, it is worthwhile to recall that the conservative scattering angle in GR [39, 40] contains a logarithmic high-energy singularity that is canceled by radiative contributions [140, 141]

$$\chi_{\text{rad.}}^{(2),\text{GR}}\Big|_{\text{HE}} = \frac{8G^3 E^3 \left(6 \log\left(\frac{E^2}{m_1 m_2}\right) - 5\right)}{3|b|^3}, \quad (4.40)$$

$$\chi_{\text{cons.}}^{(2),\text{GR}}\Big|_{\text{HE}} = -\frac{8G^3 E^3 \left(6 \log\left(\frac{E^2}{m_1 m_2}\right) - 9\right)}{3|b|^3}, \quad (4.41)$$

$$\left(\chi_{\text{cons.}}^{(2),\text{GR}} + \chi_{\text{rad.}}^{(2),\text{GR}}\right)\Big|_{\text{HE}} = \frac{32G^3 E^3}{3|b|^3} = \frac{\left[\chi_{\text{GR}}^{(0)}\Big|_{\text{HE}}\right]^3}{3!}. \quad (4.42)$$

The fact that the leading high-energy limit of the full scattering angle in gravity is given by the third power of the tree-level angle is furthermore responsible for the observed high-energy universality of gravitational scattering at $\mathcal{O}(G^3)$ [140, 141]. In comparison, for QED, only the box-sector ($\sim q_1^3 q_2^3$) angle follows the same iteration structure (see eq. (4.38)), whereas the mushroom terms (that are actually leading in the high-energy limit) do not.

Nonetheless, as was the case at one-loop order, the structure of the high-energy limit of the angle still follows a double-copy-like relation between QED and gravity under the replacement $q_i/m_i \rightarrow 1$, $m_i \rightarrow E$, and $\alpha \rightarrow G$. Notably, at two-loops in gravity, the logarithmic high-energy singularity of the individual conservative and radiative contributions to the angle is directly entangled with the mass singularity. This is due to the fact that both quantities appear linked as the argument of a logarithm $\log\frac{E^2}{m_1 m_2}$ so that one can

think about mass or high-energy divergences interchangeably. In our setup, in QED, this is no longer true, as we have explicitly seen in eqs. (4.37) and (4.36) above.

Interestingly, in the conservative sector of GR at $\mathcal{O}(G^4)$, dimensional analysis and explicit computation exposed a $1/m$ singularity [60] whose fate is unclear once radiation effects will ultimately be taken into account. Ref. [60] speculated that the $1/m$ is canceled by radiative contributions similar to the cancellation of the $\log m$ at $\mathcal{O}(G^3)$; however, it is also possible that this term remains and merely signals the breakdown of the classical massive point particle approximation which requires that $m^2 \gg |q|^2$. As such, QED seems to be an ideal toy example that exposes these features already at lower-loop order than gravity which is a consequence of the different mass dimensions of the electromagnetic (α) and gravitational (G) coupling constants. An explicit investigation of this aspect in gravity is an interesting open problem.

4.3 Radiative impulse, energy loss, and scattering angle via KMOC

Besides the eikonal analysis of the previous subsection, we have furthermore analyzed the classical two-loop scalar QED observables in the KMOC framework in complete analogy to the gravitational case that has been obtained by two of the authors [47]. Due to the linearity of QED, the present analysis is a lot simpler due to the limited number of diagrams appearing in the computation. In fact, we were able to use exactly the same analysis pipeline from before, just substituting in the new QED integrands from section 2.2.

We first assemble all relevant terms for the transverse part of the impulse, which receives both *virtual* and *real* contributions according to (2.45). Now that we are in the soft region, we do have situations where internal photons are allowed to go on-shell, so that we have to both consider two- and three-particle cuts at $\mathcal{O}(\alpha^3)$ to find

$$\begin{aligned} \Delta p_{1,\perp}^\mu = & \frac{(\alpha q_1 q_2)^3}{m_1 m_2} \left[\frac{8\sigma^2 \operatorname{arcsinh} \sqrt{\frac{\sigma-1}{2}}}{(\sigma^2-1)^{5/2}} - \frac{4\sigma^3}{(\sigma^2-1)^2} + \frac{2(2m_1 m_2 (\sigma^4 - \sigma^2 + 1) + (m_1^2 + m_2^2)\sigma)}{m_1 m_2 (\sigma^2-1)^{5/2}} \right] \frac{b^\mu}{|b|^4} \\ & + \alpha^3 q_1^2 q_2^2 \frac{4\sigma^2 (m_2^2 q_1^2 + m_1^2 q_2^2)}{3m_1^2 m_2^2 (\sigma^2-1)} \frac{b^\mu}{|b|^4}. \end{aligned} \quad (4.43)$$

In comparison to the conservative sector, we now have two different charge sectors, the one with $(q_1 q_2)^3$ dependence and the other with $q_i^2 q_j^4$. In QED, these sectors are independently gauge-invariant and do not interfere. This is distinct from the gravitational setting, where all results were proportional to G^3 which can be roughly understood from a double-copy point of view where the charges in gauge theory q_i get replaced by the gravitational charges, i.e. the masses m_i . Unlike in the conservative sector, now the $\operatorname{arcsinh} \sqrt{\frac{\sigma-1}{2}}$ appears, but is not proportional to any leading power of σ so that the ultrarelativistic limit is well-behaved. From the above result, we can subtract the conservative contribution to single out the radiative part of the impulse

$$\Delta p_{1,\perp}^{\mu,\text{rad.}} = \frac{\alpha^3 q_1^2 q_2^2}{m_1 m_2} \frac{b^\mu}{|b|^4} \left[q_1 q_2 \left(\frac{8\sigma^2 \operatorname{arcsinh} \sqrt{\frac{\sigma-1}{2}}}{(\sigma^2-1)^{5/2}} - \frac{4\sigma^3}{(\sigma^2-1)^2} \right) + \frac{4\sigma^2 (m_2^2 q_1^2 + m_1^2 q_2^2)}{3m_1 m_2 (\sigma^2-1)} \right]. \quad (4.44)$$

From the radiative transverse impulse, one can extract the radiative correction to the scattering angle [47, 99] which equally splits into different charge sectors

$$\chi_{\text{rad}}^{(2)} = \alpha^3 q_1^2 q_2^2 \frac{4\sigma^2 \left[3m_1 m_2 q_1 q_2 \left(2 \operatorname{arcsinh} \sqrt{\frac{\sigma-1}{2}} - \sigma \sqrt{\sigma^2-1} \right) + (m_2^2 q_1^2 + m_1^2 q_2^2) (\sigma^2-1)^{\frac{3}{2}} \right]}{3J^3 (\sigma^2-1)^{3/2} (m_1^2 + m_2^2 + 2m_1 m_2 \sigma)}. \quad (4.45)$$

For the longitudinal part, we only give the additional contribution due to radiation effects. In order to obtain the full longitudinal part, one would have to add the conservative result from eq. (3.41)

$$\Delta p_{1,u}^{\mu,\text{rad.}} = \frac{\alpha^3 q_1^2 q_2^2 \pi}{m_1 m_2 |b|^3} \check{u}_2^\mu \left[q_1 q_2 \frac{(3\sigma^3 - 4\sigma^2 + 9\sigma - 4) (\sigma^2 - 1) - 2(3\sigma^2 + 1) \sqrt{\sigma^2 - 1} \operatorname{arcsinh} \sqrt{\frac{\sigma-1}{2}}}{4(\sigma^2 - 1)^{5/2}} - \frac{(3\sigma^2 + 1) (m_2^2 \sigma q_1^2 + m_1^2 q_2^2)}{12m_1 m_2 \sqrt{\sigma^2 - 1}} \right], \quad (4.46)$$

where the radiative part of the momentum change on particle 1 is purely in the direction of \check{u}_2^μ . We now can compute the radiated momentum in the scattering of two charged scalars in QED in two different ways. First, we simply take the impulse on particle 1 plus the impulse on particle 2 (which can be obtained from the above results by simple relabeling) together with momentum conservation $\Delta p_1^\mu + \Delta p_2^\mu + \Delta R^\mu = 0$. Alternatively, we can directly compute the radiated momentum from KMOC, see eq. (2.47) to find

$$\Delta R^\mu = \frac{\alpha^3 q_1^2 q_2^2 \pi}{|b|^3} \left[\frac{q_1 q_2}{m_1 m_2} \frac{u_1^\mu + u_2^\mu}{\sigma + 1} \left\{ \frac{2(3\sigma^2 + 1) \operatorname{arcsinh} \sqrt{\frac{\sigma-1}{2}} - \sqrt{\sigma^2-1} (3\sigma^3 - 4\sigma^2 + 9\sigma - 4)}{4(\sigma^2 - 1)^2} \right\} + \frac{(3\sigma^2 + 1) (m_2^2 q_1^2 u_1^\mu + m_1^2 q_2^2 u_2^\mu)}{12m_1^2 m_2^2 \sqrt{\sigma^2 - 1}} \right], \quad (4.47)$$

which points entirely along the longitudinal directions u_1^μ and u_2^μ with appropriate strength proportional to the charge-to-mass ratios q_i/m_i of the scattering particles. In comparison to the GR results obtained previously [46], where the masses are always positive, the electric charges can change sign. For the $q_1^3 q_2^2$ charge sector, this implies that the contribution to the radiated energy can be positive or negative. However, the combined energy loss e.g. in the center-of-mass system

$$\Delta E_{\text{c.m.}} = \frac{\Delta R \cdot (m_1 u_1 + m_2 u_2)}{m_1 + m_2}, \quad (4.48)$$

is numerically positive for arbitrary values of the charge q_1/q_2 and mass m_1/m_2 ratios.

4.4 Radiative radial action

For completeness, we give the explicit results for the *soft radial action* for which we found an empirical shortcut in terms of explicit subtractions of master integrals that has been

described in section 2.4. Upon Fourier-transforming to impact-parameter space b , the two-loop soft radial action is

$$\begin{aligned}
 I_r^{(2)}(J, \sigma) = & \frac{(\alpha q_1 q_2)^3}{3J^2 (\sigma^2 - 1)^{3/2} (m_1^2 + m_2^2 + 2m_1 m_2 \sigma)} \left[(m_1^2 + m_2^2) \sigma (2\sigma^2 - 3) \right. \\
 & \left. - 2m_1 m_2 \left\{ 3 + (\sigma^2 - 3\sigma \sqrt{\sigma^2 - 1} - 3) \sigma^2 + 6\sigma^2 \operatorname{arcsinh} \sqrt{\frac{\sigma - 1}{2}} \right\} \right] \\
 & - \frac{2\alpha^3 q_1^2 q_2^2 \sigma^2 (m_2^2 q_1^2 + m_1^2 q_2^2)}{3J^2 (m_1^2 + m_2^2 + 2m_1 m_2 \sigma)},
 \end{aligned} \tag{4.49}$$

from which we find the scattering angle

$$\chi^{(2)} = \frac{\partial I_r^{(2)}(J, \sigma)}{\partial J}, \tag{4.50}$$

which exactly agrees with our eikonal result in eq. (4.25) and the ones that can be obtained from the impulse via the KMOC setup. At this point, our prescription for the modification of the boundary conditions for the soft master integrals was inspired by an analogous procedure in the conservative sector and it would be interesting to understand this method more systematically so that it can be applied at higher orders. It would be very interesting to find a direct computational method for the phase of the S-matrix in the representation of ref. [102] and the relation to the velocity cuts of ref. [153] as well as the heavy-particle effective theory implementation of related ideas of ref. [154].

5 Conclusions

In this paper we applied scattering amplitude techniques to study the classical two-body scattering problem in scalar electrodynamics in a regime similar to the post-Minkowskian expansion of general relativity. Scalar QED has many similarities to GR, except that it is far simpler because the underlying interactions are linear, making it useful as a toy model of the gravitational problem [33, 142]. The recent calculation of the scattering angle through $\mathcal{O}(\alpha^3)$, including radiative effects, by iteratively solving the classical equations of motion [99] motivated the computation of the corresponding results from amplitudes based approaches. We derived the classical scattering angle from both the eikonal phase [104] of the amplitude, and from the KMOC formalism [44]. We also noted a simplified computation of the radial action including radiative effects. The ‘soft radial action’ was obtained by a change in the boundary conditions of the differential equations for the soft master integrals. This automatically removes classically singular iterations and directly yields the radial action (including radiative contributions) up to two-loop order from which we obtain the classical scattering angle. All three approaches give the same scattering angle which furthermore agrees with the one found by solving the classical equations of motion [99].

An interesting feature of the scattering angle in QED is that, at $\mathcal{O}(\alpha^3)$, it contains factors of $1/m_i$ which are singular for $m_i \rightarrow 0$, despite having included both conservative and radiative effects consistently. Of course, this region is outside the validity of our setup

since it violates the classical requirement, for point particles, that the Compton wavelength is smaller than the inter-particle separation. Translated to momentum space this amounts to the classical hierarchy of scales $-q^2 \ll m_i^2$ where the masses are larger than the momentum transfer which is violated for $m_i \rightarrow 0$. The same breakdown of the approximation was found in ref. [99], where it was tied to terms generated via the ALD force [143–145]. In the classical setup, the ALD force has to be added ‘by hand’ to account for radiation loss during the scattering event. The situation in gravity is similar where an MSTQW force needs to be added [11, 12, 147]. In contrast, in amplitudes-based frameworks, the radiation loss is taken into account automatically and is on an equal footing with other terms in the amplitudes. The appearance of the mass singularities in QED may be contrasted with the corresponding $\mathcal{O}(G^3)$ scattering angle in GR: once radiative effects are included the mass singularity cancels [140, 141]. On the other hand, at $\mathcal{O}(G^4)$ the pure potential contributions to the scattering angle contain a $1/m$ singularity [60]. Our results for the electrodynamics suggest that these may not cancel even after including gravitational radiation.

Following refs. [96, 97, 99, 101] many physical observables can be analytically continued from the scattering problem to the bound-state problem. In particular, the scattering angle is directly tied to the periastron advance. In gravity, at $\mathcal{O}(G^4)$ this is greatly complicated by the nonlocal-in-time tail effect [92, 93, 95, 101, 104]. Since the tail effect arises from gravitational radiation interacting with potential gravitons (due to nonlinear graviton couplings in GR), electrodynamics should be immune from this complication, given that photons do not self interact classically in the absence of nonlinear higher derivative corrections to QED.

In summary, we expect electrodynamics to continue to serve as a useful toy model for the classical gravitational binary dynamics.

Acknowledgments

We thank Clifford Cheung, Michael Ruf, and Mikhail Solon for very enlightening discussions. We also thank Alessandra Buonanno, Justin Vines, Jan Steinhoff, and Muddu Saketh for very helpful discussions and for sharing the results of ref. [99] prior to publication, where the scattering angle is derived from the classical equations of motion. We thank Julio Parra-Martinez for discussions and comments on the manuscript. This work was supported in part by the U.S. Department of Energy (DOE) under Award Number DE-SC0009937. This project has received funding from the European Union’s Horizon 2020 research and innovation program under the Marie Skłodowska-Curie grant agreement No. 847523 ‘INTERACTIONS’. M.Z.’s work is supported by the U.K. Royal Society through Grant URF\R1\20109. We are also grateful for support from the Mani L. Bhaumik Institute for Theoretical Physics. We are grateful to the Kavli Institute for Theoretical Physics for their hospitality at the High-Precision Gravitational Waves Program, where parts of this work were carried out. This research was supported in part by the National Science Foundation under Grant No. NSF PHY-1748958.

Open Access. This article is distributed under the terms of the Creative Commons Attribution License ([CC-BY 4.0](https://creativecommons.org/licenses/by/4.0/)), which permits any use, distribution and reproduction in any medium, provided the original author(s) and source are credited. SCOAP³ supports the goals of the International Year of Basic Sciences for Sustainable Development.

References

- [1] LIGO SCIENTIFIC and VIRGO collaborations, *Observation of Gravitational Waves from a Binary Black Hole Merger*, *Phys. Rev. Lett.* **116** (2016) 061102 [[arXiv:1602.03837](https://arxiv.org/abs/1602.03837)] [[INSPIRE](#)].
- [2] LIGO SCIENTIFIC and VIRGO collaborations, *GW170817: Observation of Gravitational Waves from a Binary Neutron Star Inspiral*, *Phys. Rev. Lett.* **119** (2017) 161101 [[arXiv:1710.05832](https://arxiv.org/abs/1710.05832)] [[INSPIRE](#)].
- [3] M. Punturo et al., *The Einstein Telescope: A third-generation gravitational wave observatory*, *Class. Quant. Grav.* **27** (2010) 194002 [[INSPIRE](#)].
- [4] S. Dwyer, D. Sigg, S.W. Ballmer, L. Barsotti, N. Mavalvala and M. Evans, *Gravitational wave detector with cosmological reach*, *Phys. Rev. D* **91** (2015) 082001 [[arXiv:1410.0612](https://arxiv.org/abs/1410.0612)] [[INSPIRE](#)].
- [5] LISA collaboration, *Laser Interferometer Space Antenna*, [arXiv:1702.00786](https://arxiv.org/abs/1702.00786) [[INSPIRE](#)].
- [6] D. Reitze et al., *Cosmic Explorer: The U.S. Contribution to Gravitational-Wave Astronomy beyond LIGO*, *Bull. Am. Astron. Soc.* **51** (2019) 035 [[arXiv:1907.04833](https://arxiv.org/abs/1907.04833)] [[INSPIRE](#)].
- [7] A. Buonanno and T. Damour, *Effective one-body approach to general relativistic two-body dynamics*, *Phys. Rev. D* **59** (1999) 084006 [[gr-qc/9811091](https://arxiv.org/abs/gr-qc/9811091)] [[INSPIRE](#)].
- [8] F. Pretorius, *Evolution of binary black hole spacetimes*, *Phys. Rev. Lett.* **95** (2005) 121101 [[gr-qc/0507014](https://arxiv.org/abs/gr-qc/0507014)] [[INSPIRE](#)].
- [9] M. Campanelli, C.O. Lousto, P. Marronetti and Y. Zlochower, *Accurate evolutions of orbiting black-hole binaries without excision*, *Phys. Rev. Lett.* **96** (2006) 111101 [[gr-qc/0511048](https://arxiv.org/abs/gr-qc/0511048)] [[INSPIRE](#)].
- [10] J.G. Baker, J. Centrella, D.-I. Choi, M. Koppitz and J. van Meter, *Gravitational wave extraction from an inspiraling configuration of merging black holes*, *Phys. Rev. Lett.* **96** (2006) 111102 [[gr-qc/0511103](https://arxiv.org/abs/gr-qc/0511103)] [[INSPIRE](#)].
- [11] Y. Mino, M. Sasaki and T. Tanaka, *Gravitational radiation reaction to a particle motion*, *Phys. Rev. D* **55** (1997) 3457 [[gr-qc/9606018](https://arxiv.org/abs/gr-qc/9606018)] [[INSPIRE](#)].
- [12] T.C. Quinn and R.M. Wald, *An Axiomatic approach to electromagnetic and gravitational radiation reaction of particles in curved space-time*, *Phys. Rev. D* **56** (1997) 3381 [[gr-qc/9610053](https://arxiv.org/abs/gr-qc/9610053)] [[INSPIRE](#)].
- [13] J. Droste, *The field of n moving centres in Einstein's theory of gravitation*, *Proc. Acad. Sci. Amst.* **26** (1916) 447.
- [14] A. Einstein, L. Infeld and B. Hoffmann, *The Gravitational equations and the problem of motion*, *Annals Math.* **39** (1938) 65 [[INSPIRE](#)].
- [15] W.D. Goldberger and I.Z. Rothstein, *An Effective field theory of gravity for extended objects*, *Phys. Rev. D* **73** (2006) 104029 [[hep-th/0409156](https://arxiv.org/abs/hep-th/0409156)] [[INSPIRE](#)].

- [16] B. Kol and M. Smolkin, *Classical Effective Field Theory and Caged Black Holes*, *Phys. Rev. D* **77** (2008) 064033 [[arXiv:0712.2822](#)] [[INSPIRE](#)].
- [17] B. Kol and M. Smolkin, *Non-Relativistic Gravitation: From Newton to Einstein and Back*, *Class. Quant. Grav.* **25** (2008) 145011 [[arXiv:0712.4116](#)] [[INSPIRE](#)].
- [18] J.B. Gilmore and A. Ross, *Effective field theory calculation of second post-Newtonian binary dynamics*, *Phys. Rev. D* **78** (2008) 124021 [[arXiv:0810.1328](#)] [[INSPIRE](#)].
- [19] S. Foffa and R. Sturani, *Effective field theory calculation of conservative binary dynamics at third post-Newtonian order*, *Phys. Rev. D* **84** (2011) 044031 [[arXiv:1104.1122](#)] [[INSPIRE](#)].
- [20] S. Foffa, P. Mastrolia, R. Sturani and C. Sturm, *Effective field theory approach to the gravitational two-body dynamics, at fourth post-Newtonian order and quintic in the Newton constant*, *Phys. Rev. D* **95** (2017) 104009 [[arXiv:1612.00482](#)] [[INSPIRE](#)].
- [21] R.A. Porto and I.Z. Rothstein, *Apparent ambiguities in the post-Newtonian expansion for binary systems*, *Phys. Rev. D* **96** (2017) 024062 [[arXiv:1703.06433](#)] [[INSPIRE](#)].
- [22] S. Foffa, P. Mastrolia, R. Sturani, C. Sturm and W.J. Torres Bobadilla, *Static two-body potential at fifth post-Newtonian order*, *Phys. Rev. Lett.* **122** (2019) 241605 [[arXiv:1902.10571](#)] [[INSPIRE](#)].
- [23] J. Blümlein, A. Maier and P. Marquard, *Five-Loop Static Contribution to the Gravitational Interaction Potential of Two Point Masses*, *Phys. Lett. B* **800** (2020) 135100 [[arXiv:1902.11180](#)] [[INSPIRE](#)].
- [24] S. Foffa and R. Sturani, *Conservative dynamics of binary systems to fourth Post-Newtonian order in the EFT approach I: Regularized Lagrangian*, *Phys. Rev. D* **100** (2019) 024047 [[arXiv:1903.05113](#)] [[INSPIRE](#)].
- [25] S. Foffa, R.A. Porto, I. Rothstein and R. Sturani, *Conservative dynamics of binary systems to fourth Post-Newtonian order in the EFT approach II: Renormalized Lagrangian*, *Phys. Rev. D* **100** (2019) 024048 [[arXiv:1903.05118](#)] [[INSPIRE](#)].
- [26] J. Blümlein, A. Maier, P. Marquard and G. Schäfer, *Fourth post-Newtonian Hamiltonian dynamics of two-body systems from an effective field theory approach*, *Nucl. Phys. B* **955** (2020) 115041 [[arXiv:2003.01692](#)] [[INSPIRE](#)].
- [27] B. Bertotti, *On gravitational motion*, *Nuovo Cim.* **4** (1956) 898.
- [28] R.P. Kerr, *The Lorentz-covariant approximation method in general relativity I*, *Nuovo Cim.* **13** (1959) 469 [[INSPIRE](#)].
- [29] B. Bertotti and J. Plebanski, *Theory of gravitational perturbations in the fast motion approximation*, *Annals Phys.* **11** (1960) 169 [[INSPIRE](#)].
- [30] M. Portilla, *Momentum and angular momentum of two gravitating particles*, *J. Phys. A* **12** (1979) 1075 [[INSPIRE](#)].
- [31] K. Westpfahl and M. Goller, *Gravitational scattering of two relativistic particles in postlinear approximation*, *Lett. Nuovo Cim.* **26** (1979) 573 [[INSPIRE](#)].
- [32] L. Bel, T. Damour, N. Deruelle, J. Ibáñez and J. Martin, *Poincaré-invariant gravitational field and equations of motion of two pointlike objects: The postlinear approximation of general relativity*, *Gen. Rel. Grav.* **13** (1981) 963 [[INSPIRE](#)].
- [33] K. Westpfahl, *High-Speed Scattering of Charged and Uncharged Particles in General Relativity*, *Fortsch. Phys.* **33** (1985) 417 [[INSPIRE](#)].

- [34] T. Ledvinka, G. Schaefer and J. Bicak, *Relativistic Closed-Form Hamiltonian for Many-Body Gravitating Systems in the Post-Minkowskian Approximation*, *Phys. Rev. Lett.* **100** (2008) 251101 [[arXiv:0807.0214](#)] [[INSPIRE](#)].
- [35] T. Damour, *High-energy gravitational scattering and the general relativistic two-body problem*, *Phys. Rev. D* **97** (2018) 044038 [[arXiv:1710.10599](#)] [[INSPIRE](#)].
- [36] N.E.J. Bjerrum-Bohr, J.F. Donoghue and P. Vanhove, *On-shell Techniques and Universal Results in Quantum Gravity*, *JHEP* **02** (2014) 111 [[arXiv:1309.0804](#)] [[INSPIRE](#)].
- [37] N.E.J. Bjerrum-Bohr, P.H. Damgaard, G. Festuccia, L. Planté and P. Vanhove, *General Relativity from Scattering Amplitudes*, *Phys. Rev. Lett.* **121** (2018) 171601 [[arXiv:1806.04920](#)] [[INSPIRE](#)].
- [38] C. Cheung, I.Z. Rothstein and M.P. Solon, *From Scattering Amplitudes to Classical Potentials in the Post-Minkowskian Expansion*, *Phys. Rev. Lett.* **121** (2018) 251101 [[arXiv:1808.02489](#)] [[INSPIRE](#)].
- [39] Z. Bern, C. Cheung, R. Roiban, C.-H. Shen, M.P. Solon and M. Zeng, *Scattering Amplitudes and the Conservative Hamiltonian for Binary Systems at Third Post-Minkowskian Order*, *Phys. Rev. Lett.* **122** (2019) 201603 [[arXiv:1901.04424](#)] [[INSPIRE](#)].
- [40] Z. Bern, C. Cheung, R. Roiban, C.-H. Shen, M.P. Solon and M. Zeng, *Black Hole Binary Dynamics from the Double Copy and Effective Theory*, *JHEP* **10** (2019) 206 [[arXiv:1908.01493](#)] [[INSPIRE](#)].
- [41] A. Antonelli, A. Buonanno, J. Steinhoff, M. van de Meent and J. Vines, *Energetics of two-body Hamiltonians in post-Minkowskian gravity*, *Phys. Rev. D* **99** (2019) 104004 [[arXiv:1901.07102](#)] [[INSPIRE](#)].
- [42] A. Koemans Collado, P. Di Vecchia and R. Russo, *Revisiting the second post-Minkowskian eikonal and the dynamics of binary black holes*, *Phys. Rev. D* **100** (2019) 066028 [[arXiv:1904.02667](#)] [[INSPIRE](#)].
- [43] A. Cristofoli, P.H. Damgaard, P. Di Vecchia and C. Heissenberg, *Second-order Post-Minkowskian scattering in arbitrary dimensions*, *JHEP* **07** (2020) 122 [[arXiv:2003.10274](#)] [[INSPIRE](#)].
- [44] D.A. Kosower, B. Maybee and D. O’Connell, *Amplitudes, Observables, and Classical Scattering*, *JHEP* **02** (2019) 137 [[arXiv:1811.10950](#)] [[INSPIRE](#)].
- [45] B. Maybee, D. O’Connell and J. Vines, *Observables and amplitudes for spinning particles and black holes*, *JHEP* **12** (2019) 156 [[arXiv:1906.09260](#)] [[INSPIRE](#)].
- [46] E. Herrmann, J. Parra-Martinez, M.S. Ruf and M. Zeng, *Gravitational Bremsstrahlung from Reverse Unitarity*, *Phys. Rev. Lett.* **126** (2021) 201602 [[arXiv:2101.07255](#)] [[INSPIRE](#)].
- [47] E. Herrmann, J. Parra-Martinez, M.S. Ruf and M. Zeng, *Radiative classical gravitational observables at $\mathcal{O}(G^3)$ from scattering amplitudes*, *JHEP* **10** (2021) 148 [[arXiv:2104.03957](#)] [[INSPIRE](#)].
- [48] A. Cristofoli, R. Gonzo, D.A. Kosower and D. O’Connell, *Waveforms from Amplitudes*, [arXiv:2107.10193](#) [[INSPIRE](#)].
- [49] L. de la Cruz, A. Luna and T. Scheopner, *Yang-Mills observables: from KMOC to eikonal through EFT*, *JHEP* **01** (2022) 045 [[arXiv:2108.02178](#)] [[INSPIRE](#)].
- [50] A. Cristofoli et al., *The Uncertainty Principle and Classical Amplitudes*, [arXiv:2112.07556](#) [[INSPIRE](#)].

- [51] Y.F. Bautista and A. Laddha, *Soft Constraints on KMOC Formalism*, [arXiv:2111.11642](#) [[INSPIRE](#)].
- [52] N. Siemonsen and J. Vines, *Test black holes, scattering amplitudes and perturbations of Kerr spacetime*, *Phys. Rev. D* **101** (2020) 064066 [[arXiv:1909.07361](#)] [[INSPIRE](#)].
- [53] J. Blümlein, A. Maier, P. Marquard and G. Schäfer, *Testing binary dynamics in gravity at the sixth post-Newtonian level*, *Phys. Lett. B* **807** (2020) 135496 [[arXiv:2003.07145](#)] [[INSPIRE](#)].
- [54] C. Cheung and M.P. Solon, *Classical gravitational scattering at $\mathcal{O}(G^3)$ from Feynman diagrams*, *JHEP* **06** (2020) 144 [[arXiv:2003.08351](#)] [[INSPIRE](#)].
- [55] D. Bini, T. Damour and A. Geralico, *Binary dynamics at the fifth and fifth-and-a-half post-Newtonian orders*, *Phys. Rev. D* **102** (2020) 024062 [[arXiv:2003.11891](#)] [[INSPIRE](#)].
- [56] D. Bini, T. Damour and A. Geralico, *Sixth post-Newtonian local-in-time dynamics of binary systems*, *Phys. Rev. D* **102** (2020) 024061 [[arXiv:2004.05407](#)] [[INSPIRE](#)].
- [57] D. Bini, T. Damour and A. Geralico, *Novel approach to binary dynamics: application to the fifth post-Newtonian level*, *Phys. Rev. Lett.* **123** (2019) 231104 [[arXiv:1909.02375](#)] [[INSPIRE](#)].
- [58] G. Kälin, Z. Liu and R.A. Porto, *Conservative Dynamics of Binary Systems to Third Post-Minkowskian Order from the Effective Field Theory Approach*, *Phys. Rev. Lett.* **125** (2020) 261103 [[arXiv:2007.04977](#)] [[INSPIRE](#)].
- [59] A. Antonelli, C. Kavanagh, M. Khalil, J. Steinhoff and J. Vines, *Gravitational spin-orbit coupling through third-subleading post-Newtonian order: from first-order self-force to arbitrary mass ratios*, *Phys. Rev. Lett.* **125** (2020) 011103 [[arXiv:2003.11391](#)] [[INSPIRE](#)].
- [60] Z. Bern et al., *Scattering Amplitudes and Conservative Binary Dynamics at $\mathcal{O}(G^4)$* , *Phys. Rev. Lett.* **126** (2021) 171601 [[arXiv:2101.07254](#)] [[INSPIRE](#)].
- [61] D. Bini, T. Damour and A. Geralico, *Radiative contributions to gravitational scattering*, *Phys. Rev. D* **104** (2021) 084031 [[arXiv:2107.08896](#)] [[INSPIRE](#)].
- [62] J. Blümlein, A. Maier, P. Marquard and G. Schäfer, *The fifth-order post-Newtonian Hamiltonian dynamics of two-body systems from an effective field theory approach*, *Nucl. Phys. B* **983** (2022) 115900 [[arXiv:2110.13822](#)] [[INSPIRE](#)].
- [63] Z. Bern et al., *Scattering Amplitudes, the Tail Effect, and Conservative Binary Dynamics at $\mathcal{O}(G^4)$* , *Phys. Rev. Lett.* **128** (2022) 161103 [[arXiv:2112.10750](#)] [[INSPIRE](#)].
- [64] G. Cho, B. Pardo and R.A. Porto, *Gravitational radiation from inspiralling compact objects: Spin-spin effects completed at the next-to-leading post-Newtonian order*, *Phys. Rev. D* **104** (2021) 024037 [[arXiv:2103.14612](#)] [[INSPIRE](#)].
- [65] C. Dlapa, G. Kälin, Z. Liu and R.A. Porto, *Dynamics of binary systems to fourth Post-Minkowskian order from the effective field theory approach*, *Phys. Lett. B* **831** (2022) 137203 [[arXiv:2106.08276](#)] [[INSPIRE](#)].
- [66] C. Dlapa, G. Kälin, Z. Liu and R.A. Porto, *Conservative Dynamics of Binary Systems at Fourth Post-Minkowskian Order in the Large-Eccentricity Expansion*, *Phys. Rev. Lett.* **128** (2022) 161104 [[arXiv:2112.11296](#)] [[INSPIRE](#)].
- [67] D. Neill and I.Z. Rothstein, *Classical Space-Times from the S Matrix*, *Nucl. Phys. B* **877** (2013) 177 [[arXiv:1304.7263](#)] [[INSPIRE](#)].

- [68] Z. Bern, L.J. Dixon, D.C. Dunbar and D.A. Kosower, *One loop n point gauge theory amplitudes, unitarity and collinear limits*, *Nucl. Phys. B* **425** (1994) 217 [[hep-ph/9403226](#)] [[INSPIRE](#)].
- [69] Z. Bern, L.J. Dixon, D.C. Dunbar and D.A. Kosower, *Fusing gauge theory tree amplitudes into loop amplitudes*, *Nucl. Phys. B* **435** (1995) 59 [[hep-ph/9409265](#)] [[INSPIRE](#)].
- [70] R. Britto, F. Cachazo and B. Feng, *Generalized unitarity and one-loop amplitudes in $N = 4$ super-Yang-Mills*, *Nucl. Phys. B* **725** (2005) 275 [[hep-th/0412103](#)] [[INSPIRE](#)].
- [71] H. Kawai, D.C. Lewellen and S.H.H. Tye, *A Relation Between Tree Amplitudes of Closed and Open Strings*, *Nucl. Phys. B* **269** (1986) 1 [[INSPIRE](#)].
- [72] Z. Bern, J.J.M. Carrasco and H. Johansson, *New Relations for Gauge-Theory Amplitudes*, *Phys. Rev. D* **78** (2008) 085011 [[arXiv:0805.3993](#)] [[INSPIRE](#)].
- [73] Z. Bern, J.J.M. Carrasco and H. Johansson, *Perturbative Quantum Gravity as a Double Copy of Gauge Theory*, *Phys. Rev. Lett.* **105** (2010) 061602 [[arXiv:1004.0476](#)] [[INSPIRE](#)].
- [74] Z. Bern, J.J.M. Carrasco, L.J. Dixon, H. Johansson and R. Roiban, *Simplifying Multiloop Integrands and Ultraviolet Divergences of Gauge Theory and Gravity Amplitudes*, *Phys. Rev. D* **85** (2012) 105014 [[arXiv:1201.5366](#)] [[INSPIRE](#)].
- [75] Z. Bern, J.J. Carrasco, M. Chiodaroli, H. Johansson and R. Roiban, *The Duality Between Color and Kinematics and its Applications*, [arXiv:1909.01358](#) [[INSPIRE](#)].
- [76] J. Parra-Martinez, M.S. Ruf and M. Zeng, *Extremal black hole scattering at $\mathcal{O}(G^3)$: graviton dominance, eikonal exponentiation, and differential equations*, *JHEP* **11** (2020) 023 [[arXiv:2005.04236](#)] [[INSPIRE](#)].
- [77] F.V. Tkachov, *A Theorem on Analytical Calculability of Four Loop Renormalization Group Functions*, *Phys. Lett. B* **100** (1981) 65 [[INSPIRE](#)].
- [78] K.G. Chetyrkin and F.V. Tkachov, *Integration by Parts: The Algorithm to Calculate β -functions in 4 Loops*, *Nucl. Phys. B* **192** (1981) 159 [[INSPIRE](#)].
- [79] S. Laporta, *High precision calculation of multiloop Feynman integrals by difference equations*, *Int. J. Mod. Phys. A* **15** (2000) 5087 [[hep-ph/0102033](#)] [[INSPIRE](#)].
- [80] A.V. Kotikov, *Differential equations method: New technique for massive Feynman diagrams calculation*, *Phys. Lett. B* **254** (1991) 158 [[INSPIRE](#)].
- [81] Z. Bern, L.J. Dixon and D.A. Kosower, *Dimensionally regulated one loop integrals*, *Phys. Lett. B* **302** (1993) 299 [Erratum *ibid.* **318** (1993) 649] [[hep-ph/9212308](#)] [[INSPIRE](#)].
- [82] E. Remiddi, *Differential equations for Feynman graph amplitudes*, *Nuovo Cim. A* **110** (1997) 1435 [[hep-th/9711188](#)] [[INSPIRE](#)].
- [83] T. Gehrmann and E. Remiddi, *Differential equations for two loop four point functions*, *Nucl. Phys. B* **580** (2000) 485 [[hep-ph/9912329](#)] [[INSPIRE](#)].
- [84] J.M. Henn, *Multiloop integrals in dimensional regularization made simple*, *Phys. Rev. Lett.* **110** (2013) 251601 [[arXiv:1304.1806](#)] [[INSPIRE](#)].
- [85] J.M. Henn, *Lectures on differential equations for Feynman integrals*, *J. Phys. A* **48** (2015) 153001 [[arXiv:1412.2296](#)] [[INSPIRE](#)].
- [86] C. Anastasiou and K. Melnikov, *Higgs boson production at hadron colliders in NNLO QCD*, *Nucl. Phys. B* **646** (2002) 220 [[hep-ph/0207004](#)] [[INSPIRE](#)].

- [87] C. Anastasiou, L.J. Dixon and K. Melnikov, *NLO Higgs boson rapidity distributions at hadron colliders*, *Nucl. Phys. B Proc. Suppl.* **116** (2003) 193 [[hep-ph/0211141](#)] [[INSPIRE](#)].
- [88] C. Anastasiou, L.J. Dixon, K. Melnikov and F. Petriello, *Dilepton rapidity distribution in the Drell-Yan process at NNLO in QCD*, *Phys. Rev. Lett.* **91** (2003) 182002 [[hep-ph/0306192](#)] [[INSPIRE](#)].
- [89] C. Anastasiou, C. Duhr, F. Dulat, E. Furlan, F. Herzog and B. Mistlberger, *Soft expansion of double-real-virtual corrections to Higgs production at N^3LO* , *JHEP* **08** (2015) 051 [[arXiv:1505.04110](#)] [[INSPIRE](#)].
- [90] W. Bonnor, *Spherical gravitational waves*, *Philos. Trans. Roy. Soc. Lond. A* **251** (1959) 233.
- [91] W. Bonnor and M. Rotenberg, *Gravitational waves from isolated sources*, *Proc. Roy. Soc. Lond. A* **289** (1966) 247.
- [92] K.S. Thorne, *Multipole Expansions of Gravitational Radiation*, *Rev. Mod. Phys.* **52** (1980) 299 [[INSPIRE](#)].
- [93] L. Blanchet and T. Damour, *Tail Transported Temporal Correlations in the Dynamics of a Gravitating System*, *Phys. Rev. D* **37** (1988) 1410 [[INSPIRE](#)].
- [94] L. Blanchet and T. Damour, *Hereditary effects in gravitational radiation*, *Phys. Rev. D* **46** (1992) 4304 [[INSPIRE](#)].
- [95] L. Blanchet and G. Schaefer, *Gravitational wave tails and binary star systems*, *Class. Quant. Grav.* **10** (1993) 2699 [[INSPIRE](#)].
- [96] G. Kälin and R.A. Porto, *From Boundary Data to Bound States*, *JHEP* **01** (2020) 072 [[arXiv:1910.03008](#)] [[INSPIRE](#)].
- [97] G. Kälin and R.A. Porto, *From boundary data to bound states. Part II. Scattering angle to dynamical invariants (with twist)*, *JHEP* **02** (2020) 120 [[arXiv:1911.09130](#)] [[INSPIRE](#)].
- [98] D. Bini, T. Damour and A. Gericco, *Sixth post-Newtonian nonlocal-in-time dynamics of binary systems*, *Phys. Rev. D* **102** (2020) 084047 [[arXiv:2007.11239](#)] [[INSPIRE](#)].
- [99] M.V.S. Saketh, J. Vines, J. Steinhoff and A. Buonanno, *Conservative and radiative dynamics in classical relativistic scattering and bound systems*, *Phys. Rev. Res.* **4** (2022) 013127 [[arXiv:2109.05994](#)] [[INSPIRE](#)].
- [100] D. Bini and T. Damour, *Gravitational scattering of two black holes at the fourth post-Newtonian approximation*, *Phys. Rev. D* **96** (2017) 064021 [[arXiv:1706.06877](#)] [[INSPIRE](#)].
- [101] G. Cho, G. Kälin and R.A. Porto, *From boundary data to bound states. Part III. Radiative effects*, *JHEP* **04** (2022) 154 [[arXiv:2112.03976](#)] [[INSPIRE](#)].
- [102] P.H. Damgaard, L. Plante and P. Vanhove, *On an exponential representation of the gravitational S-matrix*, *JHEP* **11** (2021) 213 [[arXiv:2107.12891](#)] [[INSPIRE](#)].
- [103] U. Kol, D. O'Connell and O. Telem, *The radial action from probe amplitudes to all orders*, *JHEP* **03** (2022) 141 [[arXiv:2109.12092](#)] [[INSPIRE](#)].
- [104] R.J. Glauber, *Lectures in theoretical physics*, *Interscience* **1** (1959) 315.
- [105] D. Amati, M. Ciafaloni and G. Veneziano, *Higher Order Gravitational Deflection and Soft Bremsstrahlung in Planckian Energy Superstring Collisions*, *Nucl. Phys. B* **347** (1990) 550 [[INSPIRE](#)].

- [106] E. Laenen, G. Stavenga and C.D. White, *Path integral approach to eikonal and next-to-eikonal exponentiation*, *JHEP* **03** (2009) 054 [[arXiv:0811.2067](#)] [[INSPIRE](#)].
- [107] R. Akhouri, R. Saotome and G. Sterman, *High Energy Scattering in Perturbative Quantum Gravity at Next to Leading Power*, *Phys. Rev. D* **103** (2021) 064036 [[arXiv:1308.5204](#)] [[INSPIRE](#)].
- [108] Z. Bern, H. Ita, J. Parra-Martinez and M.S. Ruf, *Universality in the classical limit of massless gravitational scattering*, *Phys. Rev. Lett.* **125** (2020) 031601 [[arXiv:2002.02459](#)] [[INSPIRE](#)].
- [109] D. Bonocore, *Asymptotic dynamics on the worldline for spinning particles*, *JHEP* **02** (2021) 007 [[arXiv:2009.07863](#)] [[INSPIRE](#)].
- [110] D. Bonocore, A. Kulesza and J. Pirsch, *Classical and quantum gravitational scattering with Generalized Wilson Lines*, *JHEP* **03** (2022) 147 [[arXiv:2112.02009](#)] [[INSPIRE](#)].
- [111] T. Adamo, A. Cristofoli and P. Tourkine, *Eikonal amplitudes from curved backgrounds*, [arXiv:2112.09113](#) [[INSPIRE](#)].
- [112] J. Blümlein, A. Maier, P. Marquard and G. Schäfer, *The 6th post-Newtonian potential terms at $O(G_N^4)$* , *Phys. Lett. B* **816** (2021) 136260 [[arXiv:2101.08630](#)] [[INSPIRE](#)].
- [113] V. Vaidya, *Gravitational spin Hamiltonians from the S matrix*, *Phys. Rev. D* **91** (2015) 024017 [[arXiv:1410.5348](#)] [[INSPIRE](#)].
- [114] J. Vines, *Scattering of two spinning black holes in post-Minkowskian gravity, to all orders in spin, and effective-one-body mappings*, *Class. Quant. Grav.* **35** (2018) 084002 [[arXiv:1709.06016](#)] [[INSPIRE](#)].
- [115] A. Guevara, *Holomorphic Classical Limit for Spin Effects in Gravitational and Electromagnetic Scattering*, *JHEP* **04** (2019) 033 [[arXiv:1706.02314](#)] [[INSPIRE](#)].
- [116] J. Vines, J. Steinhoff and A. Buonanno, *Spinning-black-hole scattering and the test-black-hole limit at second post-Minkowskian order*, *Phys. Rev. D* **99** (2019) 064054 [[arXiv:1812.00956](#)] [[INSPIRE](#)].
- [117] A. Guevara, A. Ochirov and J. Vines, *Scattering of Spinning Black Holes from Exponentiated Soft Factors*, *JHEP* **09** (2019) 056 [[arXiv:1812.06895](#)] [[INSPIRE](#)].
- [118] M.-Z. Chung, Y.-T. Huang, J.-W. Kim and S. Lee, *The simplest massive S-matrix: from minimal coupling to Black Holes*, *JHEP* **04** (2019) 156 [[arXiv:1812.08752](#)] [[INSPIRE](#)].
- [119] A. Guevara, A. Ochirov and J. Vines, *Black-hole scattering with general spin directions from minimal-coupling amplitudes*, *Phys. Rev. D* **100** (2019) 104024 [[arXiv:1906.10071](#)] [[INSPIRE](#)].
- [120] M.-Z. Chung, Y.-T. Huang and J.-W. Kim, *Classical potential for general spinning bodies*, *JHEP* **09** (2020) 074 [[arXiv:1908.08463](#)] [[INSPIRE](#)].
- [121] P.H. Damgaard, K. Haddad and A. Helset, *Heavy Black Hole Effective Theory*, *JHEP* **11** (2019) 070 [[arXiv:1908.10308](#)] [[INSPIRE](#)].
- [122] R. Aoude, K. Haddad and A. Helset, *On-shell heavy particle effective theories*, *JHEP* **05** (2020) 051 [[arXiv:2001.09164](#)] [[INSPIRE](#)].
- [123] Z. Bern, A. Luna, R. Roiban, C.-H. Shen and M. Zeng, *Spinning black hole binary dynamics, scattering amplitudes, and effective field theory*, *Phys. Rev. D* **104** (2021) 065014 [[arXiv:2005.03071](#)] [[INSPIRE](#)].

- [124] D. Kosmopoulos and A. Luna, *Quadratic-in-spin Hamiltonian at $\mathcal{O}(G^2)$ from scattering amplitudes*, *JHEP* **07** (2021) 037 [[arXiv:2102.10137](#)] [[INSPIRE](#)].
- [125] A. Guevara, B. Maybee, A. Ochirov, D. O'connell and J. Vines, *A worldsheet for Kerr*, *JHEP* **03** (2021) 201 [[arXiv:2012.11570](#)] [[INSPIRE](#)].
- [126] M. Levi, A.J. Mcleod and M. Von Hippel, *N^3LO gravitational quadratic-in-spin interactions at G^4* , *JHEP* **07** (2021) 116 [[arXiv:2003.07890](#)] [[INSPIRE](#)].
- [127] M. Levi, A.J. Mcleod and M. Von Hippel, *N^3LO gravitational spin-orbit coupling at order G^4* , *JHEP* **07** (2021) 115 [[arXiv:2003.02827](#)] [[INSPIRE](#)].
- [128] W.-M. Chen, M.-Z. Chung, Y.-t. Huang and J.-W. Kim, *The $2PM$ Hamiltonian for binary Kerr to quartic in spin*, [arXiv:2111.13639](#) [[INSPIRE](#)].
- [129] Z. Liu, R.A. Porto and Z. Yang, *Spin Effects in the Effective Field Theory Approach to Post-Minkowskian Conservative Dynamics*, *JHEP* **06** (2021) 012 [[arXiv:2102.10059](#)] [[INSPIRE](#)].
- [130] A. Brandhuber and G. Travaglini, *On higher-derivative effects on the gravitational potential and particle bending*, *JHEP* **01** (2020) 010 [[arXiv:1905.05657](#)] [[INSPIRE](#)].
- [131] M. Accettulli Huber, A. Brandhuber, S. De Angelis and G. Travaglini, *Note on the absence of R^2 corrections to Newton's potential*, *Phys. Rev. D* **101** (2020) 046011 [[arXiv:1911.10108](#)] [[INSPIRE](#)].
- [132] C. Cheung and M.P. Solon, *Tidal Effects in the Post-Minkowskian Expansion*, *Phys. Rev. Lett.* **125** (2020) 191601 [[arXiv:2006.06665](#)] [[INSPIRE](#)].
- [133] G. Kälin, Z. Liu and R.A. Porto, *Conservative Tidal Effects in Compact Binary Systems to Next-to-Leading Post-Minkowskian Order*, *Phys. Rev. D* **102** (2020) 124025 [[arXiv:2008.06047](#)] [[INSPIRE](#)].
- [134] K. Haddad and A. Helset, *Tidal effects in quantum field theory*, *JHEP* **12** (2020) 024 [[arXiv:2008.04920](#)] [[INSPIRE](#)].
- [135] R. Aoude, K. Haddad and A. Helset, *Tidal effects for spinning particles*, *JHEP* **03** (2021) 097 [[arXiv:2012.05256](#)] [[INSPIRE](#)].
- [136] M. Accettulli Huber, A. Brandhuber, S. De Angelis and G. Travaglini, *Eikonal phase matrix, deflection angle and time delay in effective field theories of gravity*, *Phys. Rev. D* **102** (2020) 046014 [[arXiv:2006.02375](#)] [[INSPIRE](#)].
- [137] M. Accettulli Huber, A. Brandhuber, S. De Angelis and G. Travaglini, *From amplitudes to gravitational radiation with cubic interactions and tidal effects*, *Phys. Rev. D* **103** (2021) 045015 [[arXiv:2012.06548](#)] [[INSPIRE](#)].
- [138] C. Cheung, N. Shah and M.P. Solon, *Mining the Geodesic Equation for Scattering Data*, *Phys. Rev. D* **103** (2021) 024030 [[arXiv:2010.08568](#)] [[INSPIRE](#)].
- [139] Z. Bern, J. Parra-Martinez, R. Roiban, E. Sawyer and C.-H. Shen, *Leading Nonlinear Tidal Effects and Scattering Amplitudes*, *JHEP* **05** (2021) 188 [[arXiv:2010.08559](#)] [[INSPIRE](#)].
- [140] P. Di Vecchia, C. Heissenberg, R. Russo and G. Veneziano, *Universality of ultra-relativistic gravitational scattering*, *Phys. Lett. B* **811** (2020) 135924 [[arXiv:2008.12743](#)] [[INSPIRE](#)].
- [141] T. Damour, *Radiative contribution to classical gravitational scattering at the third order in G* , *Phys. Rev. D* **102** (2020) 124008 [[arXiv:2010.01641](#)] [[INSPIRE](#)].
- [142] A. Buonanno, *Reduction of the two-body dynamics to a one-body description in classical electrodynamics*, *Phys. Rev. D* **62** (2000) 104022 [[hep-th/0004042](#)] [[INSPIRE](#)].

- [143] H.A. Lorentz, *La théorie électromagnétique de Maxwell et son application aux corps mouvants*, *Extrait des Archives néerlandaises des sciences exactes et naturelles*. Vol. 25, EJ Brill, Leiden, The Netherlands (1892).
- [144] M. Abraham, *Theorie der Elektrizität*, BG Teubner, Leipzig Germany (1912).
- [145] P.A.M. Dirac, *Classical theory of radiating electrons*, *Proc. Roy. Soc. Lond. A* **167** (1938) 148.
- [146] C.R. Galley, A.K. Leibovich and I.Z. Rothstein, *Reply to ‘Comment on ‘Finite size corrections to the radiation reaction force in classical electrodynamics’*, *Phys. Rev. Lett.* **109** (2012) 029502 [[arXiv:1206.4773](#)] [[INSPIRE](#)].
- [147] C.R. Galley, B.L. Hu and S.-Y. Lin, *Electromagnetic and gravitational self-force on a relativistic particle from quantum fields in curved space*, *Phys. Rev. D* **74** (2006) 024017 [[gr-qc/0603099](#)] [[INSPIRE](#)].
- [148] P. Di Vecchia, C. Heissenberg, R. Russo and G. Veneziano, *The eikonal approach to gravitational scattering and radiation at $\mathcal{O}(G^3)$* , *JHEP* **07** (2021) 169 [[arXiv:2104.03256](#)] [[INSPIRE](#)].
- [149] M. Beneke and V.A. Smirnov, *Asymptotic expansion of Feynman integrals near threshold*, *Nucl. Phys. B* **522** (1998) 321 [[hep-ph/9711391](#)] [[INSPIRE](#)].
- [150] D. Kosmopoulos, *Simplifying D-dimensional physical-state sums in gauge theory and gravity*, *Phys. Rev. D* **105** (2022) 056025 [[arXiv:2009.00141](#)] [[INSPIRE](#)].
- [151] J.L. Bourjaily, E. Herrmann and J. Trnka, *Prescriptive Unitarity*, *JHEP* **06** (2017) 059 [[arXiv:1704.05460](#)] [[INSPIRE](#)].
- [152] L.D. Landau and E.M. Lifshitz, *Course of Theoretical Physics. Vol. 1: Mechanics*, third edition, Butterworth-Heinemann, Oxford, U.K. (1976).
- [153] N.E.J. Bjerrum-Bohr, L. Planté and P. Vanhove, *Post-Minkowskian radial action from soft limits and velocity cuts*, *JHEP* **03** (2022) 071 [[arXiv:2111.02976](#)] [[INSPIRE](#)].
- [154] A. Brandhuber, G. Chen, G. Travaglini and C. Wen, *Classical gravitational scattering from a gauge-invariant double copy*, *JHEP* **10** (2021) 118 [[arXiv:2108.04216](#)] [[INSPIRE](#)].
- [155] L.D. Landau and E.M. Lifshitz, *The Classical Theory of Fields*, fourth edition, Butterworth-Heinemann, Oxford, U.K. (1980).
- [156] C.R. Galley, A.K. Leibovich and I.Z. Rothstein, *Finite size corrections to the radiation reaction force in classical electrodynamics*, *Phys. Rev. Lett.* **105** (2010) 094802 [[arXiv:1005.2617](#)] [[INSPIRE](#)].
- [157] P. Forgacs, T. Herpay and P. Kovacs, *Comment on ‘Finite Size Corrections to the Radiation Reaction Force in Classical Electrodynamics’*, *Phys. Rev. Lett.* **109** (2012) 029501 [[arXiv:1202.6289](#)] [[INSPIRE](#)].
- [158] O. Birnholtz, S. Hadar and B. Kol, *Theory of post-Newtonian radiation and reaction*, *Phys. Rev. D* **88** (2013) 104037 [[arXiv:1305.6930](#)] [[INSPIRE](#)].
- [159] D. Bini and T. Damour, *Gravitational radiation reaction along general orbits in the effective one-body formalism*, *Phys. Rev. D* **86** (2012) 124012 [[arXiv:1210.2834](#)] [[INSPIRE](#)].